

**ENHANCED DEGRADATION OF PHENANTHRENE AND BENZO(A)PYRENE
IN A FIELD-CONTAMINATED SEDIMENT
INHABITED BY *ILYODRILUS TEMPLETONI*: A MICROCOSM STUDY**

A Thesis

Submitted to the Graduate Faculty of the
Louisiana State University and
Agricultural and Mechanical College
in partial fulfillment of the
requirements for the degree of
Master of Science in Chemical Engineering

in

The Department of Chemical Engineering

by

Marilou Montevirgen Nabatilan
B.S., University of the Philippines at Los Baños, 1991
M.S., University of the Philippines Diliman, 1999
May, 2006

ACKNOWLEDGEMENTS

This research was made possible by the funding support from the Hazardous Substance Research Center South and Southwest (through the HSRC Environmental Biotechnology Initiative).

Grateful acknowledgements are also due to the following....

Dr. Danny D. Reible, for serving as my major adviser, for all his patience, and for his “big” heart;

Drs. Louise J. Thibodeaux and **William M. Moe**, for the valuable comments and time serving in my committee;

Alex Kotchet and **Ravi Raghunathan**, for helping the “novice” in the lab (Environmental Lab.- Chem. Engineering);

Xiaoxia Lu and **Yonzhou Chai**, for helping me with my worms and giving attention to my questions;

Joe and Paul of the Chemical Engineering Machine Shop, who helped me in the design and fabrication of the microcosm cells.

Veronika Spevakova, who helped me with all the molecular work even during the eerie hours of night and the chilling hours of the morning;

Jessie Conty and **Lam Bui**. The intensiveness of preparing all the samples for the different analyses would not have been met, had it not for these dependable students;

My best friend, **Larry**, for simply being there with me; and our children – **Arielle**, **Joshua**, and **Miko (Miguel)**, for bearing with a student mom; and

THE WEAVER of them all!

TABLE OF CONTENTS

ACKNOWLEDGMENTS.....	ii
LIST OF TABLES.....	v
LIST OF FIGURES.....	vi
ABSTRACT.....	viii
CHAPTER	
1 INTRODUCTION.....	1
2 REVIEW OF RELATED LITERATURE	4
2.1 PAHs: Their Nature, Distribution, and Carcinogenicity.....	4
2.2 Fate and Transport of PAHs in Sediment	6
2.3 Biodegradation of PAHs.....	7
2.4 Influence of Benthic Invertebrates on PAH Fate and Transport.....	10
2.4.1 Improved Transport Regime in the Sediment	10
2.4.2 Microbial Stimulation	12
2.4.3 Bioaccumulation/Biotransformation of PAH by Invertebrates.....	13
3 MATERIALS AND GENERAL METHODOLOGY.....	14
3.1 Design and Development of Microcosm Cells	14
3.2 Test Organisms.....	17
3.3 The Sediment and Its Preparation.....	17
3.4 The Microcosm Experiment.....	18
3.5 Chemical Analyses.....	20
3.5.1 Water Content.....	20
3.5.2 PAH Analyses.....	20
3.5.2.1 PAHs in Sediment.....	21
3.5.2.2 PAHs in Worm Tissues.....	21
3.5.2.3 PAHs in Water.....	22
3.5.3 Total Organic Carbon (TOC) Analysis.....	22
3.6 Microbial Analyses.....	22
4 ASSESSMENT OF THE PHYSICO-CHEMICAL EFFECTS IN WORM- INHABITED MICROCOSMS.....	24
4.1 Introduction.....	24
4.2 Methodology.....	25
4.2.1 Description of the Microcosm Experiment.....	25
4.3 Results and Discussions.....	27
4.3.1 Temperature and Dissolved Oxygen in Feed Water.....	27

4.3.2	Survivorship, Worm Weight, and PAH in Worm Tissues.....	27
4.3.3	Dissolved Oxygen (DO) and Reduction Potential (Eh) Profiles.....	30
4.3.3.1	Dissolved Oxygen in Microcosms.....	30
4.3.3.2	Redox Potential in Sediment	36
4.3.4	PAH Flux to the Overflow Water.....	41
4.3.5	Concentrations of Phenanthrene and Benzo(a)Pyrene in the Sediment	44
4.3.5.1	Profiles of PAH Concentrations.....	44
4.3.5.2	Mass Balances.....	50
4.3.5.3	Enhanced Degradation of Phenanthrene and Benzo(a)Pyrene in Worm Microcosms.....	53
4.4	Summary and Conclusions.....	55
5	MICROBIAL ASSESMENT OF MICROCOSM SEDIMENTS BY DENATURING GRADIENT GEL ELECTROPHORESIS (DGGE): INITIAL MICROBIAL ANALYSIS.....	57
5.1	Introduction	57
5.2	Denaturing Gradient Gel Electrophoresis as a Molecular Tool in Microbial Analysis.....	58
5.3	Methodology	59
5.3.1	DNA Extraction	59
5.3.2	Polymerase Chain Reaction (PCR) Amplification	60
5.3.3	Denaturing Gradient Gel Electrophoresis	61
5.3.4	Analysis of DGGE Tracks	61
5.3.5	Quantitative Analysis of DGGE Fingerprints	62
5.4	Results and Discussions	62
5.5	Conclusions	72
6	CONCLUSIONS AND RECOMMENDATIONS	74
6.1	Conclusions.....	74
6.2	Recommendations.....	77
	REFERENCES	79
	APPENDIX: RESULTS OF PRELIMINARY SAMPLING.....	85
	VITA	90

LIST OF TABLES

Table 3.1. Some characteristics of the sediment used in the study.....	18
Table 4.1 Wet weight and tissue phenanthrene concentrations of <i>I. templetoni</i> after 97 days of exposure time.....	28
Table 4.2. Summary of calculated values for oxygen mass balances in the overlying water of microcosms.....	34
Table 4.3. Total recovery of phenanthrene and benzo(a)pyrene from the control and worm microcosms.....	50
Table 4.4 Mass balances for phenanthrene in the control (C) and worm microcosms (W).....	52
Table 4.5 Mass balances for benzo(a)pyrene in the control (C) and worm microcosms (W).....	53
Table 5.1 Depth description of samples obtained from different zones in the microcosms.....	63
Table 5.2. Dice index coefficients for comparison of control and worm microcosm.....	71

LIST OF FIGURES

Figure 2.1. Pathways of metabolic activation in the mammalian metabolism of benzo[a]pyrene. (After Hall and Grover, 1990, as cited by Sutherland et al., 1995).....	5
Figure 3.1 The microcosm cell design showing dimensions of parts.....	15
Figure 3.2 The microcosm cell showing coring accessory that allows for protrusion of the sediment from the main chamber.....	16
Figure 3.3 Experimental set up of microcosm experiment.....	19
Figure 4.1 Monitored temperature and dissolved oxygen of feed water.....	28
Figure 4.2 Oxygen concentrations in overlying water (A) and in the sediment (B) of control -C and worm - W microcosms on July 31 and October 18, 2004.	31
Figure 4.3 Oxidation-reduction potential in the sediment of worm - W microcosms on August 11 and October 11, 2004 (means \pm std deviation, n=2 measurements from two microcosms per depth).....	37
Figure 4.4 Oxidation-reduction potential in the sediment of control - C microcosms on August 11 and October 12, 2004 (means \pm std deviation, n=2 measurements from two microcosms per depth).....	38
Figure 4.5. Flux of phenanthrene to overflow water in control and worm microcosm. (means \pm std deviation, n=3 microcosms).....	42
Figure 4.6. Flux of benzo(a)pyrene to overflow water in control and worm microcosm. (means \pm std deviation, n=3 microcosms).....	43
Figure 4.7 Profile of phenanthrene concentration in the sediment (means \pm std deviation, n=2 for the control microcosms, n=3 for the worm microcosms).....	45

Figure 4.8 Profile of benzo(a)pyrene concentration in the sediment (means \pm std deviation, n=2 for the control microcosms, n=3 for the worm microcosms).....	46
Figure 4.9 Photos showing texture differences in sediment samples from the upper layers (a) and from the bottom (b).....	49
Figure 5.1 Negative image of DGGE gel (40-60% denaturant) comparing samples from two replicate worm (W) microcosms: W1 (lanes 1-8); W2 (lanes 9-16).....	65
Figure 5.2 Negative image of DGGE gel (40-60% denaturant) comparing samples from two replicate control (C) microcosms: C1 (lanes 1-8); C2 (lanes 9- 16).....	67
Figure 5.3 Negative image of DGGE gel (40-60% denaturant) comparing samples from worm microcosm 1 (W1) and control microcosm 1 (C1). Original sediment (lane 9) is also shown for further comparisons.....	68
Figure 5.4 Negative image of DGGE gel (40-60% denaturant) comparing samples from worm microcosm 2 (W2) and control microcosm 2(C2). Original sediment (lane 9) is also shown for further comparisons.....	69
Appendix A-1. Phenanthrene profile obtained from a single control and worm- treated microcosm during a preliminary coring (September, 2004).....	85
Appendix A-2. Benzo(a)pyrene profile obtained from a single control and worm- treated microcosm during a preliminary coring (September, 2004).....	86
Appendix A-3. Sediment organic carbon (TOC) in a single control and a worm- treated microcosm during a preliminary coring (September, 2004). TOC of original sediment is $6.92 \pm 0.11\%$	87
Appendix A-4. Correlation of phenanthrene with sediment organic carbon (TOC) in a worm-treated microcosm during a preliminary coring (September, 2004). TOC of original sediment is $6.92 \pm 0.11\%$	88
Appendix A-5. Correlation of benzo(a)pyrene with sediment organic carbon (TOC) in a worm-treated microcosm during a preliminary coring (September, 2004). TOC of original sediment is $6.92 \pm 0.11\%$	89

ABSTRACT

The influence of the oligochaete *Ilyodrilus templetoni* on the degradation of phenanthrene and benzo(a)pyrene present in a field-contaminated sediment was studied in microcosm experiments. Results indicate an enhanced degradation of phenanthrene and benzo(a)pyrene in microcosms inhabited by *I. templetoni*. Total phenanthrene reduction was observed at an average of 9.78 % in worm microcosms, while no reduction was observed in the control microcosms. Benzo(a)pyrene reduction, on the other hand, was determined at 78.60 % and 30.04 % in worm and control microcosms, respectively. The lowest concentrations of these PAHs at the end of 97-day study were observed well below the surface of the sediment in worm microcosms. Mass balance analysis was done based on the possible transport routes of the sediment PAHs to possibly explain the major fate pathway for phenanthrene and benzo(a)pyrene in this study. Further, the influence of the oligochaetes on the physico-chemical characteristics (specifically, redox and porewater dissolved oxygen) and the microbial characteristics of the sediment were also assessed.

Dissolved oxygen (DO) measurements indicated a limited penetration of oxygen within the 3 mm of sediment depth. Comparisons of the two sets of measurements (two months apart) indicate an increase in DO of both the worm and control microcosms. The DO increase in control microcosm was primarily due to photosynthesis on the relatively stable sediment surface. On the other hand, a larger shift in redox profile was observed in worm microcosms, at depths way beyond the penetration depth of DO. In control microcosms, although redox potential also

increased, the larger increase occurred only in the upper layers, probably due to active photosynthesis on the surface.

Molecular technique of microbiological analysis by DGGE analysis of sediment samples obtained at different depths of the microcosms suggests that the presence of the oligochaetes had influenced the microbial profile of the sediment in this study. High microbial diversity was also observed, which seem to have varied with depth in the microcosms.

CHAPTER 1

INTRODUCTION

Polyaromatic hydrocarbons (PAHs) are substances ubiquitously found in the environment and had raised concerns for their toxicity and carcinogenicity. There are over a hundred of different kinds of PAHs, and the United States Environmental Protection Agency (US-EPA) has listed 16 of them in the list of priority pollutants. For the case of solid-water environmental systems, one of the concerns is in their physico-chemical properties, which render them preferably found in the soil and sediment rather than in the water column. Although they tend to persist and get buried in the sediment through continuous deposition to the bottom, they may be redistributed to the water column due to desorption and bioturbation. Their movement up to the higher levels in the food chain through bioassimilation and bioaccumulation, are some of the routes that find PAHs to animals, humans, and the environment as a whole.

As concerns for the effects of PAH-contaminated sediments continue to grow, so are the different technologies that continue to emerge to remediate contaminated sites. One of these is bioremediation. Bioremediation is a clean-up technology, which employs microorganisms capable of degrading and/or converting hazardous substances to less potent products. Bioremediation, as a tool, has proven to be a practical and cost-effective on-site alternative for dealing with contaminated environments. A lot of research has been done in this field in an effort to discover new viable technologies and further improve efficiency and reduce costs of

implementation of existing ones. However, still a lot need to be probed. In an effort to contribute to the field of bioremediation, this research may be geared towards the possible macrobenthos-mediated biodegradation of contaminants, PAH in particular, and its potential as a strategy in bioremediation of PAH-contaminated sediments, parallel to the technology of phytoremediation.

Earlier experiments done in our laboratory suggest the enhanced degradation of PAHs in the presence of macrobenthos. Maranto (1996), in her accounting of the different fates of sediment PAHs, reported of increased amount of “missing” contaminants with higher population of worms in the test sediment. Cunningham (2002), also reported of higher removal of laboratory-inoculated pyrene in the worm-treated sediment. Both of these experiments have realized significant contribution of microbial degradation as a fate mechanism for the PAHs in the sediment. However, the mechanisms of interaction between the worms and the microbes were not analyzed. The microbial characteristic of the sediment itself, as a response to the presence of the macrobenthos was not investigated.

The purpose of this research was to provide initial observations on the influence of the small oligochaete worms (*Ilyodrilus templetoni*) on the degradation of PAHs (phenanthrene and benzo(a)pyrene) in a field contaminated sediment. It particularly aims to evaluate the interaction between *I. templetoni* and the indigenous microorganisms in the PAH-contaminated sediment with respect to phenanthrene and benzo(a)pyrene degradation. Since the influence of vertical-feeders like *I. templetoni* may be a function of depth in the sediment, PAH analysis had to be done at thin

(~ 1mm in the upper layers, to about 1 cm thickness in the lower layers) sections in the sediment. A design and development of a microcosm was therefore one of the initial activities which needed to be accomplished. Changes in concentrations of phenanthrene and benzo(a)pyrene were followed at different depths in the microcosms and efforts to explain the results were done by assessing the influence of the oligochaetes on some physico-chemical and microbiological parameters of the sediment. Physico-chemical aspects of this interrelationship may include pore water dissolved oxygen and redox potential as functions of depth in the sediment. Microbiological parameters may include microbial density profile, diversity, and functions, which may require such molecular microbiological techniques as denaturing gradient gel electrophoresis (DGGE), real-time polymerase chain reaction (PCR) and reverse transcription polymerase chain reaction (RT-PCR). Reported herein are the results of DGGE analysis only.

This study is expected to generate results that will give us better understanding of how degradation of PAHs in the sediment is influenced by the presence of macrobenthic organisms. This understanding may find its relevance in evaluating the overall fate and transport of PAHs in contaminated sediments inhabited by benthic organisms. Since quantification of contaminant transport pathways is an essential element of sediment management, it may also aid in management approaches for clean-up requirements of these sites. Initial results could also aid in the assessment of the potential of macrobenthos-enhanced bioremediation, parallel to what phytoremediation had accomplished.

CHAPTER 2

REVIEW OF RELATED LITERATURE

2.1. PAHs: Their Nature, Distribution, and Carcinogenicity

Polyaromatic hydrocarbons (PAHs), otherwise known as polynuclear aromatic hydrocarbons (PNAs), are a group of over a hundred organic compounds known for their toxicity and environmental persistence. They are made up of carbon and hydrogen assembled in stable two or more benzene rings. They are present as natural constituents in fossil fuels and are formed during incomplete combustion of fuels like coal, oil and gas. They may come from such natural sources as forest fires and volcanic eruptions or from variety of other anthropogenic sources, which may include industrial effluents and seepages, and spillages of petrochemical products.

PAHs occur ubiquitously in the environment and are widely distributed in both the aquatic and terrestrial environments. However, their structure renders them of low aqueous solubility and of hydrophobic character. They are, therefore, most likely found bound in soils and the sediments. They may also bioaccumulate in the food chain, preferably in the fatty tissues of animals. Frequently, the PAHs are also encountered as constituents of non-aqueous phase liquids (NAPLs), which make them largely unavailable to microorganisms.

PAHs have been known for their carcinogenicity. They have been extensively studied and found to induce tumors in experimental animals. High levels of PAHs in water and sediments have been implicated in tumor development in fish (Herbes, 1977). Many PAHs, including benzo[*a*]pyrene (b[*a*]p), are known to function as

precarcinogens that require metabolic activation before they are able to bind to DNA, RNA, or proteins (Kadlubar and Hammons, 1987; Hall and Grover, 1990, as cited by Sutherland et al., 1995). For example, in the case of b[a]p, its activation as an ultimate carcinogen requires the catalytic oxidation (by cytochrome P₄₅₀ monooxygenase enzyme) of the terminal benzo ring to form benzo[a]pyrene 7,8-diol-9,10 epoxide, which was found to have four stereoisomers (Figure 2.1). Of these isomers, studies of DNA binding, bacterial mutagenesis, and mammalian tumorigenesis have shown that the isomer benzo[a]pyrene (+)-7,8-diol-9,10-epoxide-2 is the most potent ultimate carcinogen produced from benzo[a]pyrene in mammalian metabolism (Sutherland et al., 1995).

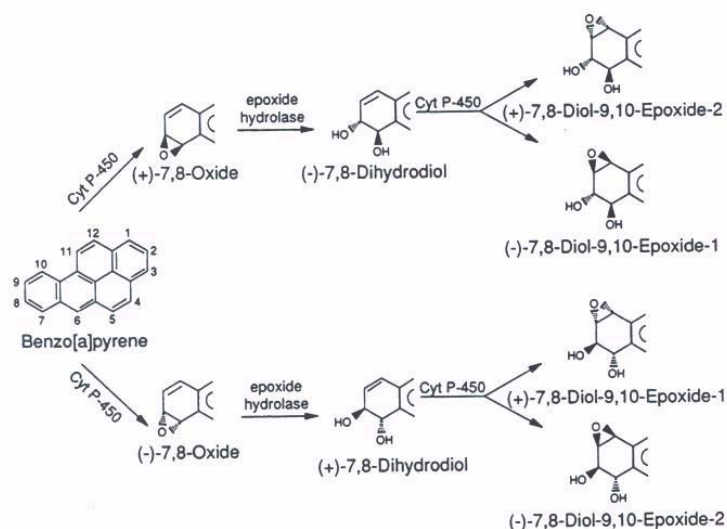


Figure 2.1. Pathways of metabolic activation in the mammalian metabolism of benzo[a]pyrene. (After Hall and Grover, 1990, as cited by Sutherland et al., 1995).

For humans, the possible hazards associated with exposure to PAHs include cancer, skin problems, immunodeficiencies, and reproductive problems. Numerous epidemiologic studies have also shown a clear association between exposure to various mixtures of PAHs containing benzo[*a*]pyrene and increased lung cancer. No direct association between benzo[*a*]pyrene alone and lung cancer has been reported. Based on US-EPA guidelines, benzo[*a*]pyrene was assigned to weight-of-evidence group B2, a probable human carcinogen, and is therefore classified as a priority pollutant.

2.2 Fate and Transport of PAHs in Sediment

PAHs are found in all the different environmental matrices – air, water, soil or sediment - at different concentrations. They may be found in smaller amounts in the air than in the sediment and may primarily be considered as a problem of the soil or sediment matrix. They tend to bind onto the organic carbon in the soil/sediment because of their hydrophobic nature.

There are different pathways of PAH mobility in the sediment. Their ultimate fate is controlled by the balance between these competing pathways. In general, these pathways may include either or combinations of the following:

- a) Diffusion. PAHs may move from the sediment to the overlying water due to a gradient in concentration between the sediment porewater and the overlying water. Diffusive fluxes are characterized by the diffusivity constant.
- b) Advection. Advective fluxes are due to bulk flow between the sediment and the overlying water.

- c) Resuspension. Resuspension of solids from the sediment surface results from the shearing effect of the fluid velocity near the sediment. Otherwise known as erosive fluxes, particle scoured from the surface of the sediment would carry sorbed PAHs.
- d) Transformations and Degradation. Transformations and degradation of PAHs in the sediment are mediated either by the microorganisms and some macrobenthic organisms.
- e) Photodegradation. Although this pathway may not usually be important in deep aquatic systems, it may be of particular concern when the above pathways are enhanced, resulting to substantial amounts of PAHs into the water column where light penetration could be possible. In one study of Fasnacht and Blough (2002) on aqueous photodegradation of PAHs, they calculated rate constants for photodegradation in an optically-thin section of surface waters during the summertime at mid-latitude varied from a low of $3.2 \times 10^{-7} \text{ hr}^{-1}$ for fluorene to a high of 7.6 hr^{-1} for benzo[a]pyrene.

2.3 Biodegradation of PAHs

Microbial degradation represents the major route responsible for the ecological recovery of PAH-contaminated sites. This route however poses challenges to researchers who would like to pursue research on this area.

The persistence of PAHs poses particular problems for microorganisms. PAH molecule stability and hydrophobicity are two primary factors which contribute to the persistence of PAHs in the environment (Kanaly and Harayama, 2000). For instance,

the more benzene rings there are, the more stable is the molecule. As a rule, PAHs with four or five rings are highly persistent (Alexander, 1999). Bioremediation projects are actually limited to the lower-molecular-weight PAHs, say, for up to four benzene rings. Beyond the four benzene rings, as is the case with benzo[*a*]pyrene, there is no report of mineralization using the PAH as the sole carbon and energy source. The degradation of larger PAHs probably results from co-metabolic reactions that occur very slowly in a natural environment. On the other hand, the hydrophobic nature of PAHs reduces their bioavailability to the microorganisms. This follows from the traditional paradigm of microbial degradation, which occurs via three steps – 1) desorption from the organic matrix in the soil or sediment; 2) dissolution into the water phase; and 3) diffusion through the microbial cell wall. However, until recently, it was generally thought that microorganisms utilize PAHs as substrates in their dissolved phase (Wattiau, 2002). Thomas, et al. (1986) suggested that direct uptake from sorbed or crystalline PAHs can also be an important mechanism during PAH degradation. Other factors on which biodegradability of PAHs in the environment may also depend include their concentration, as well as such environmental factors as soil type and condition, temperature, and pH.

Reports on PAH biodegradation are also generally limited to aerobic conditions. Lack of accumulation of oxygenated metabolic intermediates in sediments containing larger PAHs supports the hypothesis of Herbes and Schwall (1978) that the rate limiting steps in catabolic aerobic degradation of PAHs is the initial ring oxygenation and that intermediate intracellular metabolites are further oxidized

almost as rapidly as they are produced. Aerobic degradation rates of PAHs in marine sediments are typically slow and microbial degradation is primarily thought to be limited by the concentration of PAHs solubilized in the aqueous phase (Bosma et al., 1997; Harms and Bosma, 1997). Furthermore, molecular oxygen is essential to catalyze the initial oxygenation by microorganisms (Cerniglia and Heitkamp, 1989). Microorganisms play an important role in the recycling of elements such as carbon, nitrogen and phosphorous and this activity quickly depletes oxygen. The rate of oxygen consumption thus generally exceeds the rate at which oxygen can be replenished (Fenchel et al., 1996).

Anaerobic biodegradation of PAHs is another area of research on PAH biodegradation that is less understood. As cited in Holmer et al. (1997), only a few bacteria are found capable of anaerobic degradation of PAH (Berry et al., 1987; Evans and Fuchs, 1988; Myers et al., 1994). Low molecular weight PAHs are known to undergo microbial degradation under anaerobic but only a few studies have demonstrated degradation of larger PAHs under anaerobic conditions (Coates et al., 1996; Coates et al., 1997; Zhang and Young, 1997). There are also only a few reports of anaerobic degradation of complex mixtures of PAHs and the capacity to degrade PAHs is most likely the result of previous long-term exposure to high concentrations (Coates et al., 1997).

Both bacteria and fungi have been studied and observed to degrade polyaromatic hydrocarbons. Lower molecular-mass PAHs, like phenanthrene and naphthalene are readily degraded by a wide range of different microorganisms which use them as sole source of carbon and energy. However at present, there are a limited

information regarding the bacterial biodegradation of PAHs with five or more benzene rings. Benzo(a)pyrene and other PAHs with high molecular masses were observed to have occurred in mixed cultures or under co-metabolic conditions. This describes the relative difficulty of degrading benzo[a]pyrene and other high-molecular-weight PAHs for use as the sole carbon and energy source .

2.4 Influence of Benthic Invertebrates on PAH Fate and Transport

Several studies that associate benthic organisms to evaluations of fate and transport of organic matter and contaminants have been done. It has been recognized that benthic infauna can have substantial influence on the character and nature of sediment. For instance, this influence of benthic invertebrates has been attributed either to their feeding behavior or through bioturbation due to such activities as burrowing, structure building, and displacement. In the following subsections, focus is on the influences of benthic invertebrates on the fate and transport of some sediment-associated compounds, and are herein grouped into three categories:

- improved transport regime in the sediment;
- microbial stimulation; and
- biotransformation

2.4.1 Improved Transport Regime in the Sediment

Sediment particles and associated compounds within certain depths in the sediment are in active transport due to bioturbation. Bioturbation is defined as the sediment processing by animals during burrowing, sediment ingestion/defecation, tube building, and biodeposition (Reible, et al., 1996). During the process, sediment

may be resuspended to the overlying water, transported some other positions, and or buried deeper into the sediment. A conveyor-belt feeding invertebrate for instance, would burrow head down, ingest sediment, pass it along the length of its body, and out of its posterior end/tail partially exposed to the water for oxygenation. Should associated contaminants come out unaltered, they would now have better chances of being redistributed to the water column. Another possibility would be bioirrigation of burrows that brings the contaminants in better proximity to the overlying water. These result in an increased flux of contaminants from the sediment and are collectively termed as bioturbative flux. Several studies (Reible, 1996) have shown that this flux due to bioturbation is some orders of magnitude higher than in non-bioturbated sediment. Conversely, transport of materials deeper into the sediment is also a consequence of worm activities in the sediment. Myers et al. (1994) observed the burial of fluoranthene deeper into the anaerobic layers, which may have limited its degradation and loss from the sediment. Mermillod-Blondin et al. (2004), in a microcosm experiment, studied the relative influence of bioturbation and predation on organic matter processing in river sediments. In their experiments, both with and without gammarids, bioturbation by the tubificids modified both the distribution of surface particles in the sediment column and water flux. The activity of worms led to a higher penetration of luminophores into the sediment in comparison with control and gammarid only treatments.

In several studies, the more sought after effects of benthic organisms are on the sediment redox and oxygen concentrations. This is probably so because these are usually associated with increased degradation of contaminants and which are usually

an important objective of most studies. The reworking of sediment by deposit-feeding benthic macrofauna is observed to extend the depth of aerobic layer in the sediment (Fenchel, 1996). This ventilation of the sediment through burrow irrigation with oxygenated water has been associated to increased degradation of contaminants in the sediment. Repetitive oscillations of redox have also been observed (Aller, 1994) and which have shown to stimulate organic matter decomposition.

2.4.2 Microbial Stimulation

The benthos may influence not only the physical and chemical characteristics of the sediment, but also the microbiota (Aller, 1988; van de Bund, Goedkoop and Johnson, 1994; Hansen and Kristensen, 1997; Stief and de Beer, 2002). Microbial stimulation by the benthic macrofauna can either be direct or indirect. Indirect stimulation could result from an improved region due to ventilation and burrow activities (Aller, 1982; Kristensen, 1988). This improved region, as earlier mentioned, is characterized by increased oxygen concentration and redox that provides for a conducive environment for microbial activities. Benthic organisms may also indirectly stimulate microbial populations by modulating the availability of resource flows and facilitation of solute transport.

Directly, microbial stimulation can be considered to be due to the feeding activities of the macrofauna. Animals could modify microbial activity by feeding on bacteria and thus keeping them in an active physiological state (Yingst & Rhoads, 1980, as cited in Mermillod-Blondin, et al., 2004).

2.4.3 Bioaccumulation/Biotransformation of PAH by Invertebrates

Bioaccumulation studies on benthic invertebrates are many. However, biotransformation studies are limited. The ability of benthic invertebrates to metabolize and transform PAHs has been demonstrated in a few species (Geissing, 2003). Forbes et al. (1996), as cited by Holmer, 1997, showed that *Capitella* sp. I is capable of metabolizing fluoranthene, such that tissue concentrations of PAH decreased to below detection after about the fourth day of exposure to concentrations up to 350 ppm. These metabolic processes by the invertebrates involve a two-phase process which include initial addition of the OH⁻ to the hydrophobic, lipid-soluble parent PAHs and addition of carbohydrate or sulfate moiety to form soluble conjugates – glucoside, glucuronide, and sulfate conjugates (Geissing, 2003).

CHAPTER 3

MATERIALS AND GENERAL METHODOLOGY

3.1 Design and Development of Microcosm Cells

To meet the objectives of the research, a microcosm cell design was accomplished that will allow for microcosm experiments that may require coring of the sediment for investigations of effects on sediment PAHs, on water content, on organic carbon, and on microbial diversity and functions, at different depths of the sediment.

The design of the microcosm cell as shown in Figure 3.1 has a T-shape construction, which consists of the main chamber to contain the sediment, and the shoulder through which water flows. The bottom of the main chamber has a movable plate that could be locked to its place by an o-ring seal. This seal also prevents leakage to and from the main chamber. On the shoulders are two ports for water inlet and outlet, which were constructed to be at the same level as the sediment surface during the run of the experiment. The flowing water on top of the sediment is maintained at a height of 3 centimeters using a dam construction near the outlet. The whole design includes a coring tool, which basically consists of a rotating shaft that could be attached to the movable bottom plate of the cell during sampling (Figure 3.2). The rotating mechanism pushes up the bottom plate by a millimeter for each complete turn of the shaft. This results to corresponding protrusion of the sediment out from the main chamber of the microcosm, which could then be scraped off and

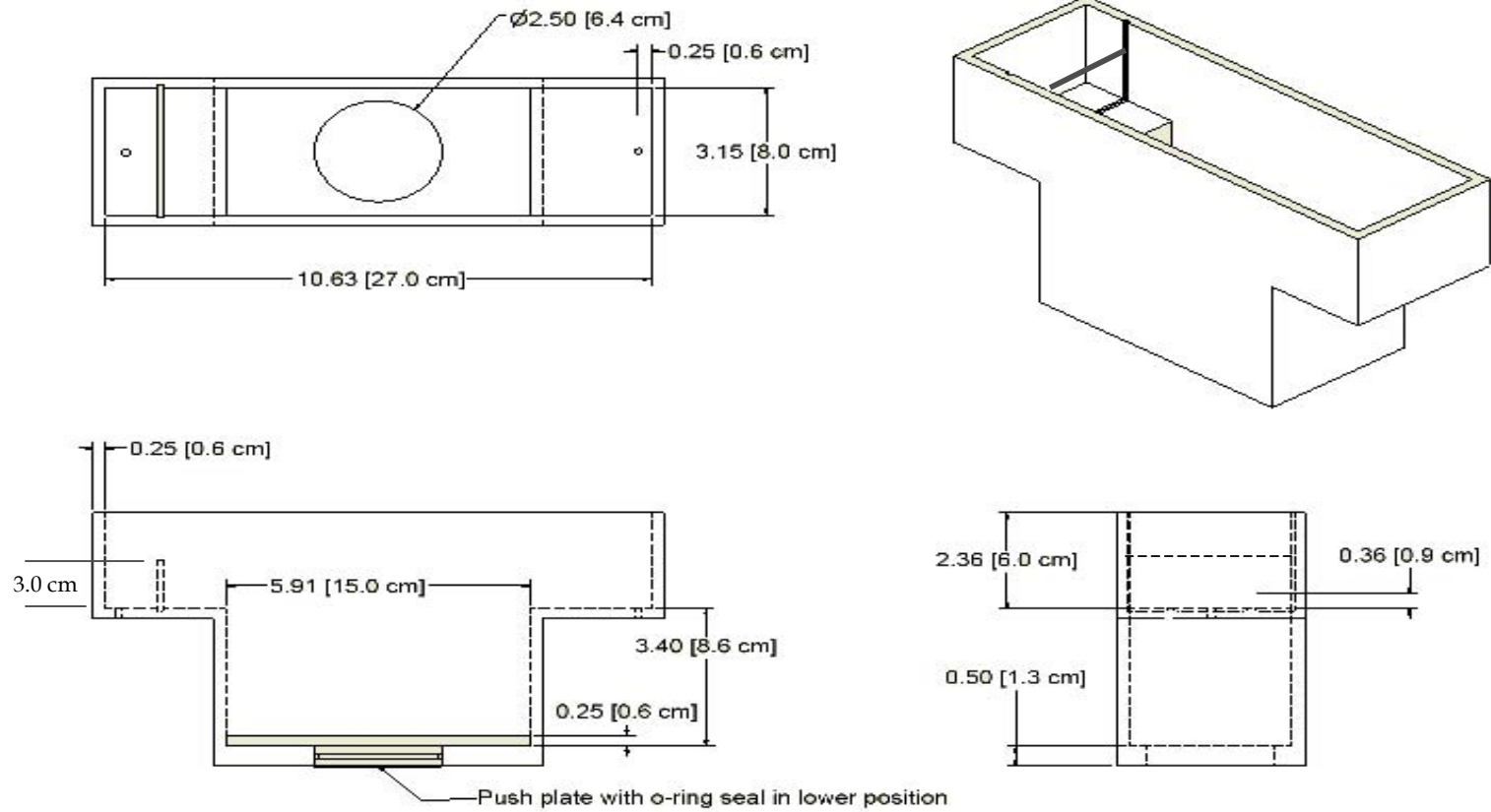


Figure 3.1 The microcosm cell design showing dimensions of parts.

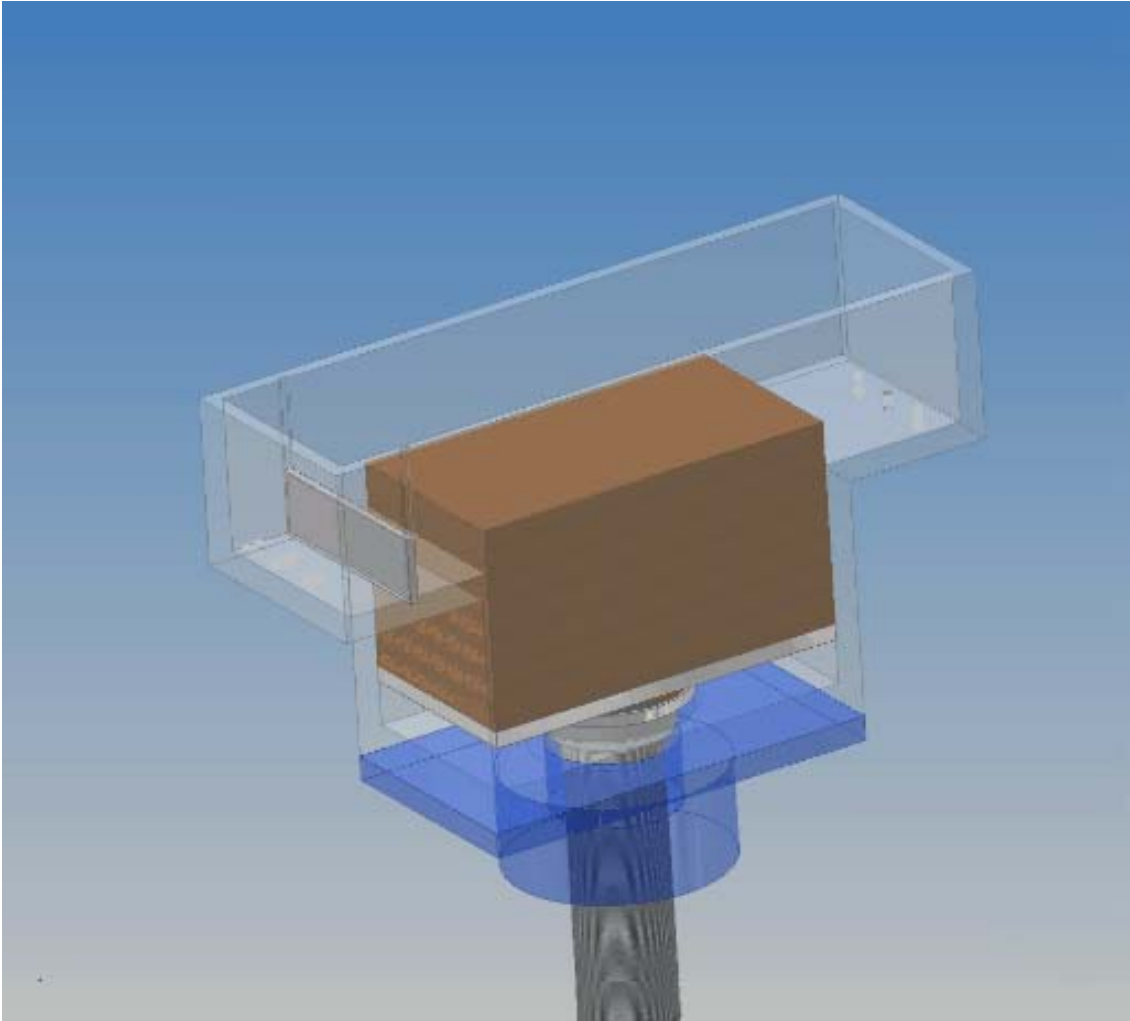


Figure 3.2 The microcosm cell showing coring accessory that allows for protrusion of the sediment from the main chamber.

collected as a sediment sample representing particular depth from the surface of the sediment column.

All the microcosm cells, as well as the coring tool, were fabricated in the LSU Chemical Engineering Machine Shop.

3.2 Test Organisms

The oligochate *Ilyodrilus templetoni* are the test organisms used in this study. They were reared in laboratory culture in 2.5-liter aerated aquaria at room temperature, fed with commercially available worm food. The worms were characterized with an average length of 2-5 cm and an average wet weight of about 3 mg.

Worms collected before and after the experiment were analyzed for wet weight, moisture, and PAH. Worms collected at the end of the experiment, however, were depurated in clean water for about 24 hours before analyses. Wet weight was determined from worm samples blotted dry on KimWipes using a balance (APX-60, Denver Instrument; d=0.1 mg). Worm tissue concentrations of PAHs were analyzed by HPLC of samples directly extracted with acetonitrile.

3.3 The Sediment and Its Preparation

The sediment used for this study was obtained from Anacostia River (Washington, D.C.) collected and provided to our laboratory by Horne Engineering and Services. It is a surficial sediment (0-6 inches) obtained using ponar sampler. In the laboratory, the sediment was passed through 2mm sieves to remove large materials like twigs, leaves, broken glasses, and stones. Until further use, the

sediment was stored in the laboratory at room temperature. Pertinent characteristics of this sediment determined after sieving are presented in Table 3.1.

Table 3.1. Some characteristics of the sediment used in the study. *

	Concentration
f_{oc} (fraction of total organic carbon)	$6.92 \pm 0.11\%$
Phenanthrene	3.02 ± 0.27 mg/kg dry sediment
Benzo(a)pyrene	3.70 ± 0.23 mg/kg dry sediment

* Values are means (\pm standard deviation from the mean). f_{oc} calculations were based on 2 replicate samples; PAH concentrations, based on 5 replicate samples.

3.4 The Microcosm Experiment

Using the designed and fabricated cells described above, a microcosm experiment was conducted and is referred to hereafter as “microcosm experiment”. This experiment basically consisted of either worm-inhabited or no-worm sediment with continuously overflowing water on top of the sediment through the shoulders of the cells. Overflow water coming from the cells was treated prior to discharge by adsorption onto a granular activated carbon column. The schematic of the set-up is shown in Figure 3.3.

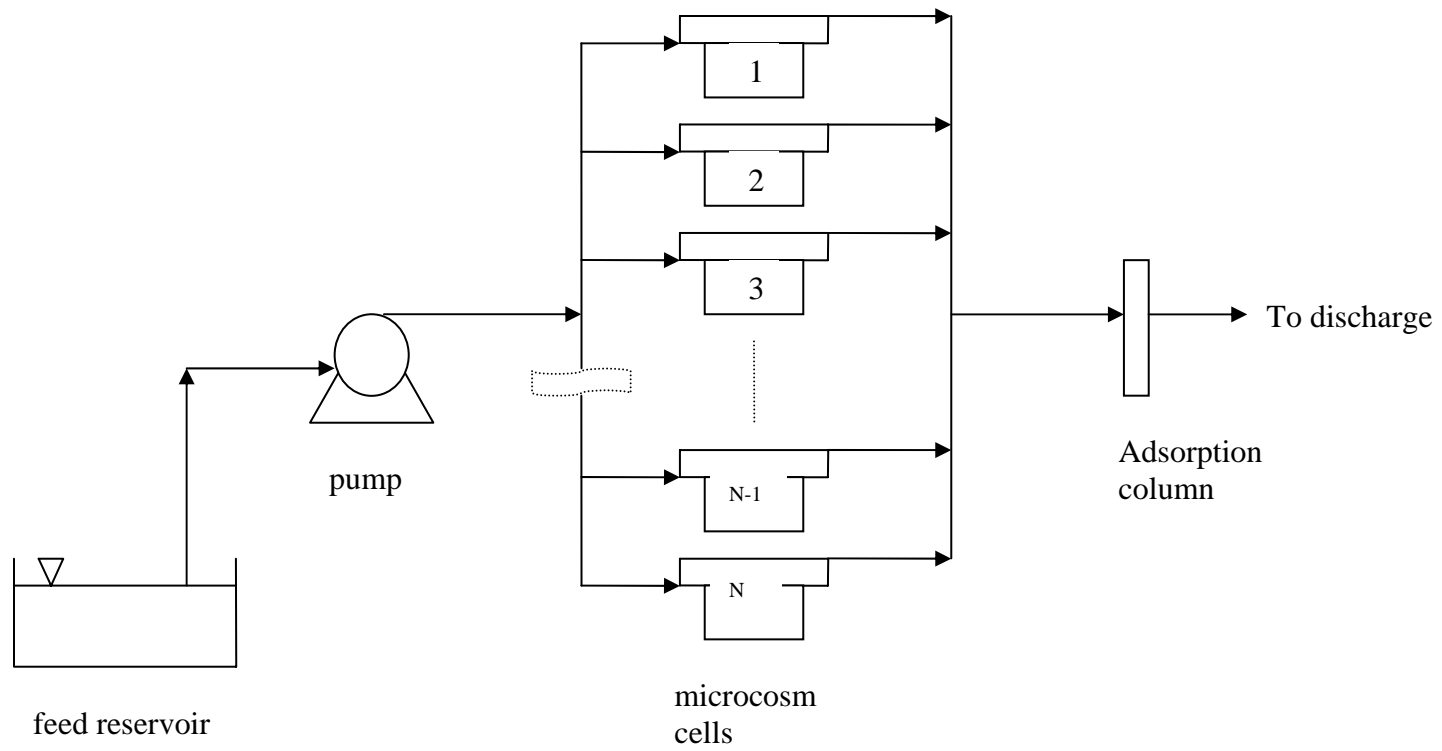


Figure 3.3. Experimental set up of microcosm experiment.

During the course of the experiment, feed water temperature and DO; overflow water and wastewater PAHs; sediment redox potential and oxygen, were measured. Then after 97 days, the same experimental cells were sliced for sampling. Samples were obtained from the center of each of the slices for chemical and microbiological analysis. Chemical analyses done include sediment PAH analysis, with water content analysis. Microbiological analyses include DNA extraction, polymerase chain reaction (PCR) amplification, and the denaturing gradient gel electrophoresis (DGGE).

3.5 Chemical Analyses

3.5.1 Water Content

About 10g of samples of the diluted and tumbled sediments were added in pre-weighed, 25-mL vials. The initial weight of vial with the sediment was determined and placed in an oven (105-110°C) overnight for drying. After drying, the final weight of the vial and dried sediment was again determined and the difference in the values of the weights corresponds to the water content of the sediment. This was done in duplicate.

3.5.2 PAH Analyses

Glasswares used in any PAH analyses were thoroughly cleaned by soaking in 10% chromium acid bath for at least 24 hours. These were then washed with tap water and rinsed with metal-free de-ionized water. Drying was done at 300°C in an oven specifically used for drying purposes of cleaned glasswares.

3.5.2.1 PAHs in Sediment

Samples of the original sediment and those sliced from the control and worm-treated cells (97 days treatment) were first extracted with a solvent. Extracts were then analyzed for PAH by chromatographic methods as modified from the EPA method (EPA Methods 610, U.S. EPA). About 1 to 2 grams of the sediment sample were mixed with 20g of anhydrous sodium sulfate to dry the sediment. Lumps of dry sediment-sodium sulfate mixture were crushed before 60mL of 50/50 (v/v) hexane/acetone mixture was added. The mixtures were then sonicated for 20 minutes in a 20°C water bath. Two mL of the extraction solvent was transferred to 2-mL tubes and allowed to evaporate under a stream of pure nitrogen to about 0.2mL of concentrated sample. Acetonitrile was added to fill to 2 mL of mixture and analyzed for PAH using a Hewlett Packard 1100 series high performance liquid chromatograph (HPLC, Hewlett Packard, Palo Alto, CA, USA) with UV-Diode array detector and fluorescence detector. For later analysis, samples in acetonitrile were stored in the refrigerator at 4°C for a maximum of one week.

3.5.2.2 PAHs in Worm Tissues

The body burden of phenanthrene and b[a]p in worms were determined by a procedure similar to that of the sediment. About 7-10 individual worms were pat-dry on Kimwipes and weighed in 20-mL glass vials. About 20 grams of Na₂SO₄ were added to further dry the worms. Using a metal spatula, the worm tissues were ground and further broken down. About 4-6 mL of dichloromethane (DCM) was then added

to extract the PAH. The extract was solvent-exchanged with ACN and the final mixture analyzed by HPLC described above.

3.5.2.3 PAHs in Water

PAHs in water sampled from the feedwater, the overflow water, and the wastewater from the carbon adsorption column were determined by the method modified from EPA. Collected samples of about 500 mL were extracted of PAHs using 10 mL hexane. The mixtures were placed in a shaker for 20 minutes and sonicated for 20 minutes in a sonicator-water bath maintained at 20°C. The solvent hexane was exchanged with acetonitrile and analyzed by HPLC.

3.5.3 Total Organic Carbon (TOC) Analysis

Sediment total organic carbon (TOC) was analyzed in the Coastal Studies Institute, LSU. Samples were first dried overnight and ground in our laboratory. Further treatments were then done in the Coastal Studies Institute, LSU. Samples were treated with 1 N HCl for carbonate removal and re-dried. About 15 mg sediment was taken for TOC analysis in a Perkin Elmer 2400 series II CHN elemental analyzer (Perkin Elmer Corporation, Norwalk, CT, USA). Two replicates per sample were analyzed. TOC is reported as fraction of the total mass of the sediment.

3.6 Microbial Analyses

Microbiological analyses on the molecular basis were done on the cored sediment. Two to four grams of samples from each of the slices were taken and stored at -20°C for until further analysis. Changes in microbial profiles were determined by denaturing gradient gel electrophoresis (DGGE) of amplicons after polymerase chain

reaction (PCR) amplification of DNA extracts. Details of these analyses are given in Chapter 5.

CHAPTER 4

ASSESSMENT OF THE PHYSICO-CHEMICAL EFFECTS IN WORM-INHABITED MICROCOSMS

4.1 Introduction

Evidence of enhanced degradation of organic matter in the sediment as influenced by benthos have been reported. These observations have been explained by the influence that the benthos have on the characteristics and diagenetic processes in the sediment, as well as on the microbiotic characteristics of the sediment. Few studies, however, are available with regards to polyaromatic hydrocarbon degradation as influenced by benthos. We therefore have some limited understanding of the mechanisms by which these benthic organisms could enhance the degradation process. The focus in this chapter is on the oligochaete *I. templetoni* and the physico-chemical aspects of its influence on the degradation of phenanthrene and benzo(a)pyrene in a field-contaminated sediment.

Initial observations expected in this work are the profiles of phenanthrene and b[a]p degradation as influenced by the oligochaetes. The observations were focused upon contrasting the profiles of phenanthrene and b[a]p degradation in the presence of oligochaetes to profiles in their absence in order to infer potential impacts on transport and degradation. Physico-chemical aspects like dissolved oxygen and redox potential were also determined to help to elucidate the profiles of degradation observed. Different transport pathways for the PAHs were also assessed to be able to identify contaminant fate in the sediment. The oligochaete *I. templetoni* is a bulk-

deposit feeder that ingests sediment at depth and defecates at the sediment surface. Profiling of parameters that describe sediment characteristics at different depths was done based on the premise that the influence of *I. templetoni* may vary with depth in the sediment.

4.2 Methodology

4.2.1 Description of the Microcosm Experiment

Initial preparation for the microcosm experiment includes preparation of the microcosm cells themselves. Each of the cells was soaked in deionized water for one week and dried. This is a recommended procedure for bioaccumulation studies employing plastic microcosms for the worms. After soaking and drying, each was sanitized by wiping the inner surfaces with 70% EtOH solution and dried again. The cells were then weighed and filled to a height of 8.6 cm, corresponding to the height of the main chamber in the cell. Care was taken to get the sediment height at the same level as the “shoulder” of the cell so as to minimize delocalization of water within the main chamber as water flows through the shoulder. Such delocalization may limit the supply of oxygen to the worms in the sediment of the main chamber. The sediment-bed was allowed to consolidate in the cell overnight before the initiation of the experiment. Since consolidation overnight may cause some reduction in the height of the sediment column, sediment was added again the following day to maintain it at level with the shoulder of the cell.

Initiation of the experiment was carried out with the introduction of 250 worms to each of the nine microcosm cells. These are identified as the worm-treated

microcosm cells. Five other cells were taken as controls (no worms). As soon as the worms were introduced to the sediment, aerated water was fed continuously to the cells at 5 mL/min with a multi-channel peristaltic pump. This was accomplished by providing two feed water reservoirs: a main drum, where the pump directly withdraws water for delivery to the different cells; and another one that was filled and aerated to standby (shown earlier in Figure 3.3). As the main drum gets depleted of its contents, it is refilled with water from the other drum. Effectively, the procedure of long standing the water while in both drums would have been able to aerate the water, release chlorine from the water, and stabilize temperature to room condition. The experiment was performed at laboratory temperature of 23 ± 1 °C.

During the course of the experiment, feed water temperature and DO were monitored using the Model YSI 55 dissolved oxygen meter (YSI Inc., Ohio, USA). The probe is provided with both temperature and DO measurement. The overflow water and wastewater from the adsorption column were monitored for PAH on a daily basis during the first week, and on a weekly or biweekly basis from then on. The sediment from the control and worm-treated cells were monitored for redox potential and dissolved oxygen (DO). The DO in the sediment (as well as in the overlying water) was monitored with a Clark-style oxygen microelectrode (Diamond General, Ann Arbor, MI) attached to a chemical microsensor for oxygen measurement. Redox profiles of the sediment were determined using a combination redox needle electrode (Diamond General, Ann Arbor, MI). Both the DO and the redox at different depths in

the sediment were measured with the aid of a micromanipulator, which enables us to draw down the electrodes by a fraction of millimeter into the sediment.

After 97 days, the sediment in the different cells (3 worm cells and two control cells) were sliced by 1 mm thickness for the first 10-12 mm from the surface, and by 5 mm thickness for the rest of the sediment. Only the results of analyses from three worm cells and two control cells are reported here. The rest of the cells were allowed to run for longer time. Each of the slices of sediment was weighed and then sampled from the middle of the slice for chemical and microbiological analysis. Methods of chemical analyses are as previously described.

4.3 Results and Discussions

4.3.1 Temperature and Dissolved Oxygen in Feed Water

Aerated water continuously flowed through each cell at about 4.5-5mL/min. The temperature and dissolved oxygen concentration of the feed water into the cells were monitored and are summarized for the first 52 days in Figure 4.1. Temperatures of the feed water before refill (DO_{feed}) and after refill (DO_{refill}) were within 1°C difference in values. On the other hand, dissolved oxygen of the feed water rises from a low value of about 6.2 mg/L during refill, to about 7.3 mg/L prior to the next refill. Lowest DO concentration was monitored at 67% saturation.

4.3.2 Survivorship, Worm Weight, and PAH in Worm Tissues

Worms with minimum length of about 2 cm were collected in one of the cells at the end of the 97 days. Almost all of the worms (247 of 250) were recovered. This confirms an earlier count obtained during the preliminary sampling (done a month

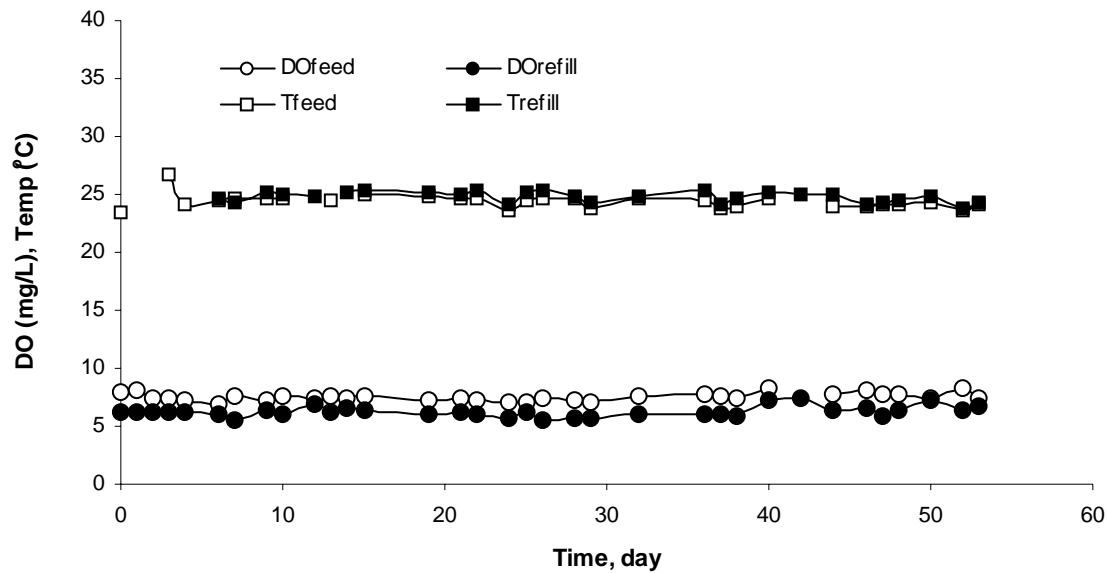


Figure 4.1 Monitored temperature and dissolved oxygen of feed water.

earlier than this sampling) when about 94% of the worms were recovered from one of the cells.

The worm weight increased significantly ($p < 0.05$) by an average of 59.2% (Table 4.1). This increase in weight of the worms reflects the favorable nature of the sediment for worms' growth.

Table 4.1 Wet weight and tissue phenanthrene concentrations of *I. templetoni* after 97 days of exposure time. *

Sampling Time	Wet Weight (mg)	Tissue Phenanthrene (mg/kg dry wt)
Initiation of experiment (t = 0)	2.70 (\pm 0.36)	Not detected
End of experiment (t = 97 days)	4.29 (\pm 0.51)	1.16 (\pm 0.11) (BSAF=0.242)**

* means (\pm standard deviation); n= 5 groups of 7-10 worms for wet weight and tissue phenanthrene concentration.

** BSAF = biota-sediment accumulation factor

Phenanthrene and benzo(a)pyrene in worms' tissues were determined after gut purging for 24 hours. Tissue concentrations of phenanthrene at the end of the experiment was determined at 1.16 ± 0.11 mg/kg worm dry weight. This concentration of phenanthrene is relatively low compared to the values obtained by Lu, et al (2003) with 15-day exposure of *I. templetoni* in desorbed (after two to three isopropanol washings) sediments of similar phenanthrene loading (i.e., 2.87 and 4.42 mg/kg dry wt sediment, with observed tissue phenanthrene concentrations of 9.63 and 17.20 mg/kg dry wt worms, respectively). This difference could be due to the difference in the sediment used itself. In this study, a field-contaminated sediment was used, with phenanthrene probably being less available to the oligochaetes. Hence, the lower bioaccumulation of phenanthrene even with the longer exposure of the oligochaetes in the sediment. The corresponding biota-sediment accumulation factor (BSAF) for phenanthrene was also determined at an average value of 0.242, based on the average lipid fraction of 0.11 (earlier determined in our laboratory for worms exposed to Anacostia River sediment for about 30 days) and the sediment phenanthrene and organic carbon concentrations already shown. This BSAF value for phenanthrene is also smaller than what was observed by Lu (2003) from the desorbed (after two to three isopropanol washings) laboratory-inoculated sediments. In her work, she reported an average BSAF value of 0.59, which is about half of the corresponding value for that of the reversibly-sorbed (labile) phenanthrene she observed.

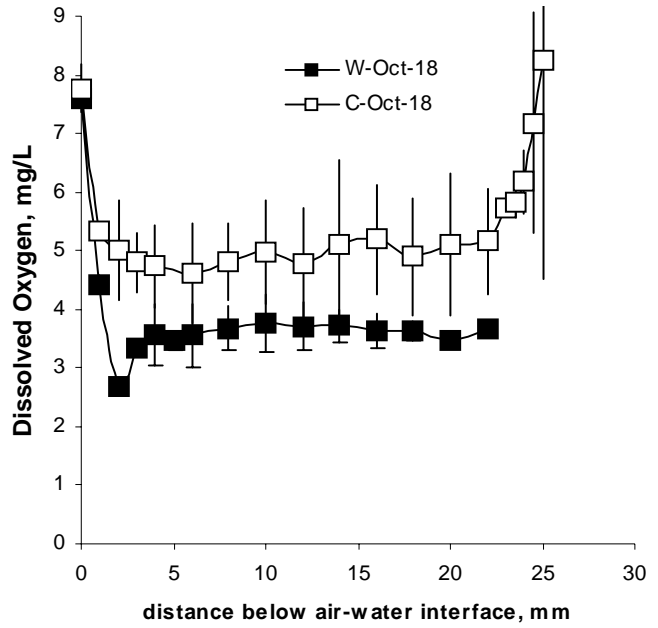
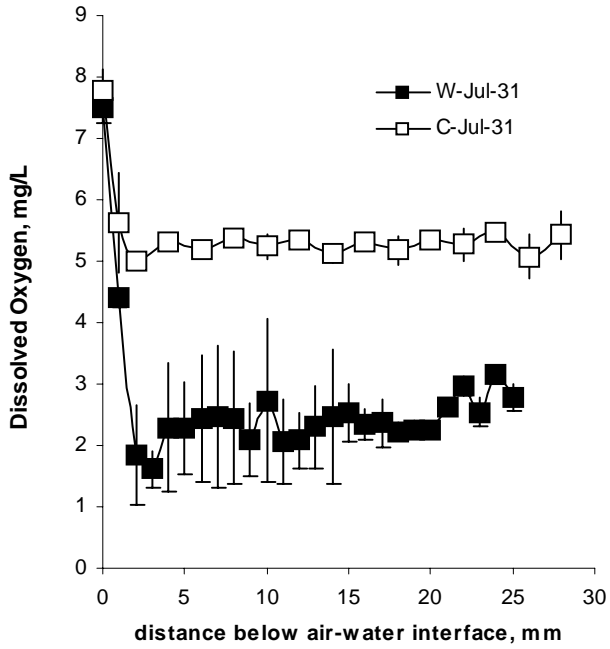
Benzo(a)pyrene was not detected in the worm bodies after 24 hours of gut purging. It is either that the elimination of benzo(a)pyrene was rapid or that the accumulation of benzo(a)pyrene by these worms is not significant. Again, the limited availability of benzo(a)pyrene to the worms could be a key factor.

4.3.3 Dissolved Oxygen (DO) and Reduction Potential (Eh) Profiles

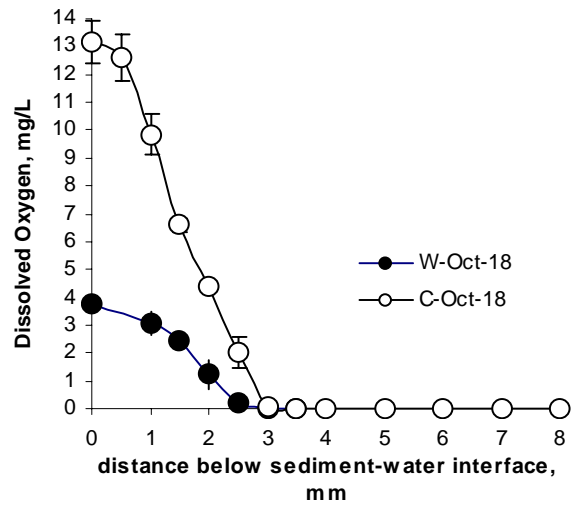
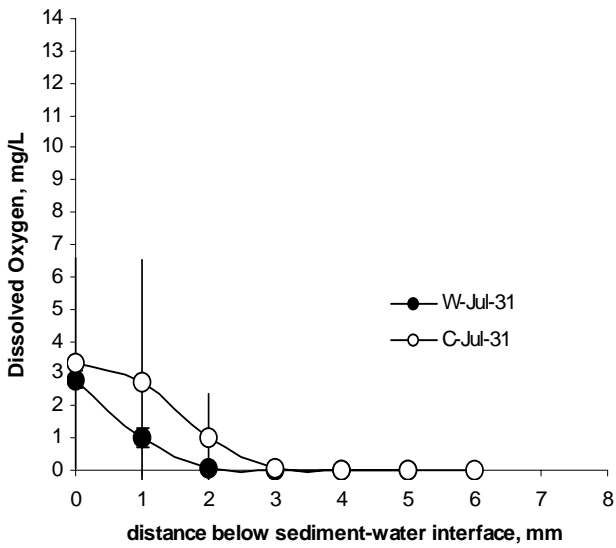
4.3.3.1 Dissolved Oxygen in Microcosms

Profiles of oxygen concentration in the overlying water and in the surficial sediments of the microcosms from the water surface in the microcosms were determined on two instances (July 31, 2004 and October 18, 2004). Measurements were split to present profiles in the water only and in the sediment only (see Figures 4.2A and 4.2B). Control microcosms had overlying water DO, which remained relatively constant at about 5 mg/L during those two measurements, except during the later measurement when the DO concentrations increased at points approaching the sediment surface. This increase in DO concentrations near the sediment surface is attributed to the growth of algae on the relatively undisturbed sediment surface in the control microcosms. As will be discussed further later, this was not observed in the worm microcosms, where the sediment was constantly turned and worked by the oligochaetes. In the worm microcosms, the water DO concentration profile slightly changed with a general increase in DO concentrations of about 1 mg/L at each of the water depths considered. These concentrations, however, remained lower than those in the controls.

Profiles of DO concentrations in the sediments also changed. Sediment DO in



A



B

Figure 4.2 Oxygen concentrations in overlying water (A) and in the sediment (B) of control -C and worm -W microcosms on July 31 and October 18, 2004.

the worm microcosms increased from a maximum of 2.8 mg/L during the earlier measurement, to about 3.8 mg/L during the later measurement. On the other hand, sediment DO concentration in the control increased from a maximum of 3.3 mg/L to a maximum value of 13.1 mg/L. All of these maximum values were observed at or very near the sediment surface. In both the control and the worm microcosm, penetration depth of DO did not significantly change during the two measurements. Apparent in the figures are penetration depths of about 2 mm during the initial measurement, which increased to about 3mm after approximately 2-½ months in worm microcosms. In the control microcosms, penetration depth of DO was limited to 3 mm during both measurements. It is important to note here that initially, DO has penetrated deeper into the control sediment than in the worm microcosm, probably because oxygen is being consumed by the presence of the worms before it can penetrate farther down into the sediment. This penetration depth increased after about 2 1/2 months, however, possibly due to effective pumping of oxygen-containing overlying water into their burrows. As for the control microcosm, DO penetration depth did not increase even if very high DO levels have developed (due to algal photosynthesis) near the sediment surface. While oxygen penetration in the worm microcosms may have been limited by the availability of DO in the overlying water due to the additional consumption of oxygen by the worms, in the control microcosm we have seen the effect of a limited diffusion even at very high oxygen concentration in the overlying water near the sediment surface.

Oxygen concentrations in the overlying water of the microcosms differed between treatments even though oxygen supplied with the feed water was already

near saturation at the room temperature. The observed low values in worm microcosms could be due to significant consumption of oxygen by the worms themselves, as already mentioned, or due to increased oxygen demand because of enhanced mixing activities of the organisms. Roughly, the difference in the amount of oxygen transported to the sediment in the worm microcosm and in the control microcosm is equivalent to the consumption by the worms. Although no data are available to account for the respiration rate of the oligochaetes, attempt to determine this, was done by an oxygen balance in the microcosm cells, as shown below. A comparison with existing data for *Limnodrilus hoffmeisteri* was also done, as will be shown later. Physically, *Limnodrilus hoffmeisteri* are similar to *I. templetoni*. They are ~1 mm in diameter and commonly grow to a length of roughly 2-4 cm (Brinkhurst, 1970).

The removal rates of DO from the flowing water in both the controls and the worm-treated microcosms was computed from the DO mass balances around the cells, assuming negligible other sources for oxygen.

$$\text{Flow in} - \text{flux out of the water to sediment} - \text{flow out} = 0 \quad \text{Eq'n 4.1}$$

$$Q C_o - k_s A C_c - Q C_c = 0 \quad (\text{control}) \quad \text{Eq'n 4.1a}$$

$$Q C_o - k_w A C_w - Q C_w = 0 \quad (\text{worm-treated}) \quad \text{Eq'n 4.1b}$$

Where

Q = flowrate of water through the cell, mL/min;

C_o = initial oxygen concentration in the feedwater, mg/L;

A = sediment surface area, cm^2 ;

C_c, C_w = oxygen concentration in the overlying water of control and worm microcosm, respectively, mg/L; and
 k_s, k_w = oxygen transfer rate constant to the control and worm sediment, respectively, cm/min.

The flow rate was taken at an average value of 4.5 mL/min with an initial oxygen concentration equivalent to the average feed water concentration of 6.86 mg/L. Sediment surface area was 120 cm² (8 cm x 15 cm top area of the sediment chamber). Oxygen concentrations in the overlying water in the control and worm microcosms were taken from two sets of measurements (July 31, 2004 and October 18, 2004). Results of calculations are summarized in Table 4.2 below.

Table 4.2. Summary of calculated values for oxygen mass balances in the overlying water of microcosms.

Date	Control Microcosm		Worm Microcosm	
	C_c , mg/L	k_s , cm/min	C_w , mg/L	k_w , cm/min
July 31, 2004	5.21 ± 0.19	1.19E-02	2.42 ± 0.53	6.88E-02
Oct. 18, 2004	5.25 ± 0.55	1.15E-02	3.54 ± 0.27	3.52E-02

The rates of oxygen transport to the control sediment (k_s) are significantly lower than those in worm microcosm. These remained constant with constant

concentration of dissolved oxygen in the overlying water. In worm microcosms, k_w was reduced to about half the initial value while DO in the overlying water increased by about 1 mg/L (as shown earlier).

If the respiration rate of the oligochaetes can be approximated from the difference in oxygen flux to the sediment between the control ($k_s \times C_c$) and the worm microcosms ($k_w \times C_w$), these values would be 0.072 and 0.044 mg O₂/worm-day on July 31, 2004 and on October 18, 2004, respectively. These values were compared to that obtained by Cunningham (2002) after recalculation of Beck's (1972) data for *Limnodrilus hoffmeisteri*. Cunningham (2002) reported a value of 3.71×10^{-4} mg O₂/worm/hr, which can be converted (on a dry mass basis) to 1.24×10^{-3} mg O₂/mg dry worm/hr, based on the dry weight of mature *L. hoffmeisteri* averaging 0.3 mg (Brinkhurst, 1970). The values obtained in this work with *I. templetoni* are 4.76×10^{-3} and 2.91×10^{-3} mg O₂/mg dry worm-hr on July 31, 2004 and on October 18, 2004, respectively (wet weight =3 mg; dry weight ~21%). These values are thereby reasonable approximations of the actual respiration rate of *I. templetoni*.

As earlier mentioned, the calculated respiration rates are rough estimates because these values also account for possible increase in the sediment oxygen demand effected by bioturbation. The decrease in respiration rate of the oligochaetes could be due to some decrease in the activities of the worms. Although these activities were actually observed to occur from an initial state of restlessness to a less agitated state, the actual time of transition is not known. During the earlier measurement, the worms were observed to have kept on waving their posteriors in the water in a more vigorous manner than they did during the later measurement when most of them were

burrowed down in the sediment. In a restless state, they are expected to breathe more and use up more oxygen. Also, higher sediment oxygen demand may have resulted because of increased bioturbation.

The increase in sediment DO of the worm microcosm is hereby attributed to the bioventilation of worm burrows due to pumping of higher oxygen-containing water on top of the sediment. Larger increase of oxygen at the surface of control sediment was observed and must be due to apparent active photosynthetic process on the sediment surface. Algal mat of about 2-3 mm thickness was observed in the control microcosms. Note that a huge increase in DO was observed in the overlying water of the control as it nears the sediment surface. The high DO gradient between the water near the surface and the pore water may have increased transport of oxygen within its penetration depth in the control sediment. The algal growths were not observed with the worm cells where the worms were present, continuously processing the surface of the sediment.

4.3.3.2 Redox Potential in Sediment

Shown in Figure 4.3 and Figure 4.4 are the redox profiles of the sediment in the worm-treated and the control microcosms, respectively. The values are averages obtained from the same depth in two representative microcosms corrected for the use of Ag/AgCl as reference electrode. Profiles were obtained at two points in time, about two months apart (from August 11 to October 11/12, 2004).

During the first measurements, reduction potentials at all depths in the control microcosms are greater than the corresponding potentials at the same depths in the

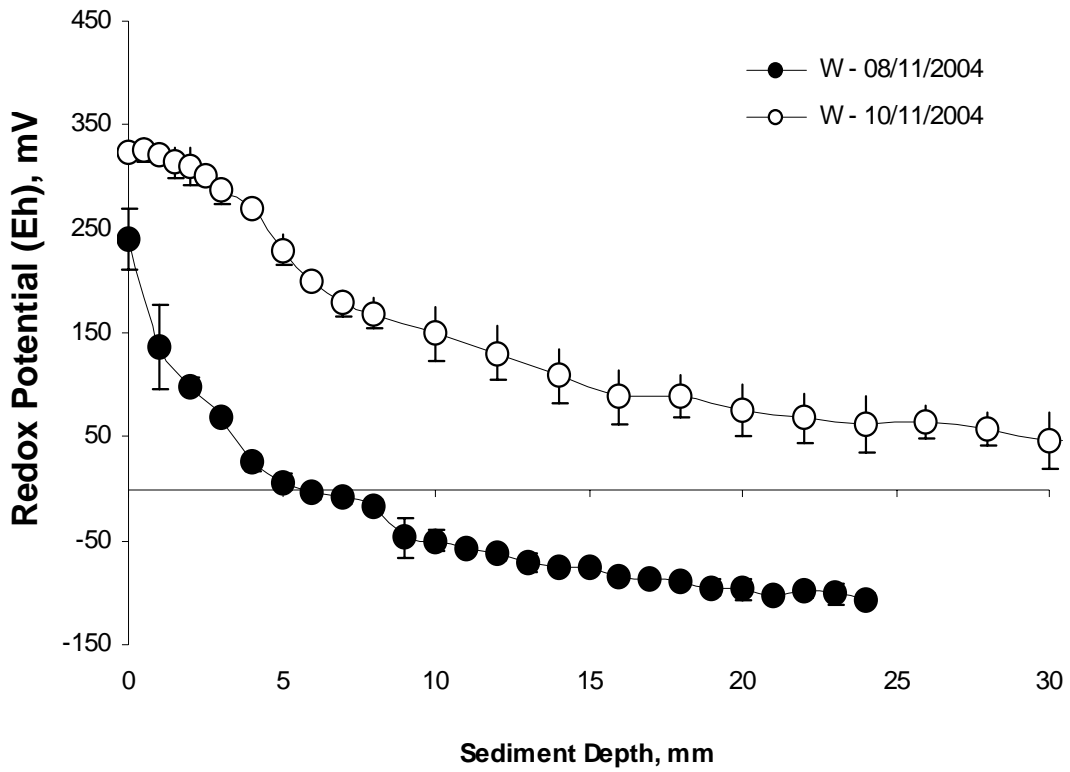


Figure 4.3 Oxidation-reduction potential in the sediment of worm-W microcosms On August 11 and October 11, 2004 (means \pm std deviation, n=2 measurements from two microcosms per depth).

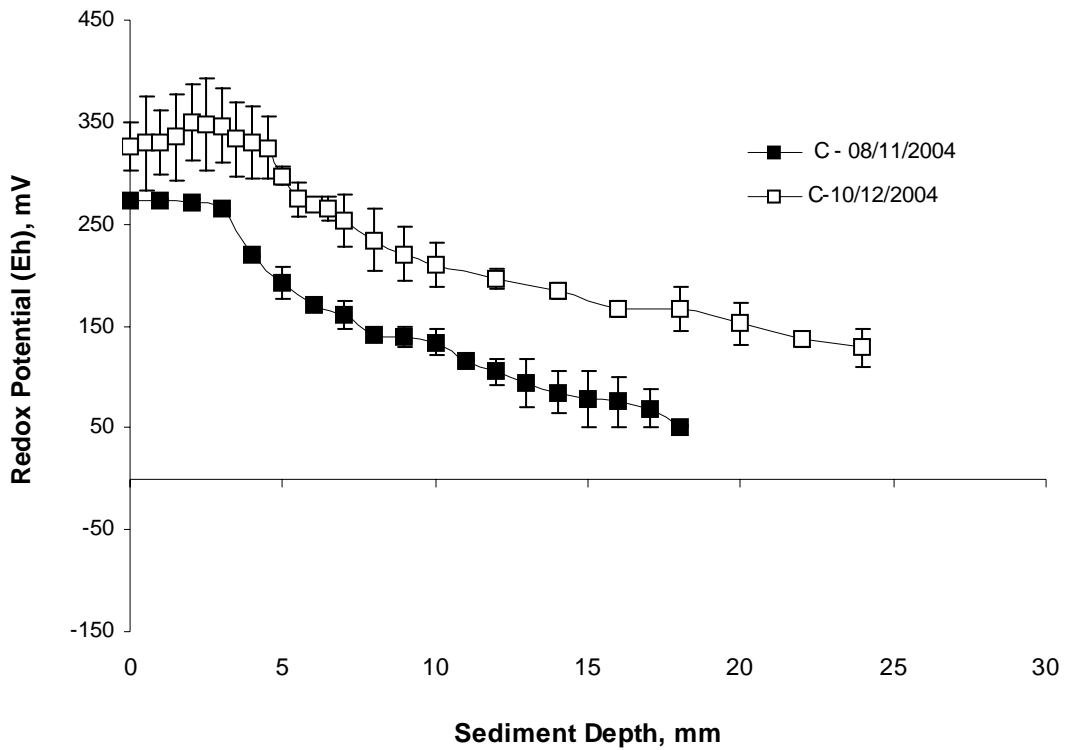


Figure 4.4 Oxidation-reduction potential in the sediment of control- C microcosms on August 11 and October 12, 2004 (means \pm std deviation, n=2 measurements from two microcosms per depth).

worm-treated microcosms. Sediment in worm microcosm was moderately reduced with positive potentials only in the upper 5mm of the sediment. Control microcosms had positive Eh values at all depths considered in the measurement, although only the first 3 or the first 4 mm may be considered moderately aerobic. Aerobic conditions are usually described with potentials of +500mV, moderately aerobic at about +250 mV, and anaerobic for negative potentials (Pardue et al.,1988).

The controls are in the moderately reduced state at most depths, true for both measurement times (August 11 and October 12, 2004). Based on the redox values, it may be assumed that most likely, iron and manganese oxides are the electron acceptors being used as electron acceptors in those depths. $\text{Fe}(\text{OH})_3$ and MnO_2 are oxides very common in soils and sediments (Hemond and Fechner, 1994). This may also be the case in worm microcosms, except during earlier measurements when sulfate reduction may be the initial dominating reaction in lower depths (probably beyond the 10-25 millimeter from the sediment surface). It is not quite easy to detect the chemical species involved in the reduction-oxidation process as the demarcation line on the redox scale that distinguishes one oxidizing species from another is not definite, due in part to variability in reactant/product concentrations. Actual measurements of reacting species may therefore have to be done to be able to have a clearer understanding of the redox reactions occurring in the sediment.

During the two sets of measurements, a shift of profile was observed in both microcosms. An average increase of about 187 mV per depth was measured in worm microcosms. On the other hand, an average increase of about 68 mV per depth was

observed in the control microcosms, primarily contributed by values at points near the surface (2-5 mm from the surface). Hence, the worms were able to effectively change the redox profile of the sediment. A more dramatic shift in redox profile occurred with the bioturbated than with the control sediment even though algal oxygenation on the surface of the controls was expected to have considerably changed its redox profile.

The shifts in the redox profiles do not very well reflect the sediment DO profiles earlier described. While DO increased within some limited depths in the sediment, the redox potential in the sediment of worm microcosms increased well below these depths. Similar results were obtained by Foster and Graf (1992) in their study of the changes in redox potential influenced by oxygen penetrating from burrows of a burrowing shrimp, *Callinasa subterranean*. Oxygen penetrated up to 1 mm by diffusion from burrow walls into the adjacent sediment, whereas elevated Eh values were measured within 3 mm of the burrow.

It may seem that DO itself is a less “sensitive” parameter than redox potential when studying impacts and effects of worms on the sediment. This is because oxygen can be limited by its diffusion through the sediment. It is important to note here though that oxygen may have actually been transported as pulses deeper into the sediment, but could not be detected in cumulative amount as it may be used up as soon as it is pumped into the sediment during the reworking of the worms. Hence, the DO may not be detected deeper in the sediment, while the effect on redox could be measured way below the penetration depths of oxygen. These results hereby suggest

that the stimulation pattern of redox potential in the sediment by the oligochaetes can not be explained by a simple extension of the oxic layer in the sediment.

4.3.4 PAH Flux to the Overflow Water

The concentrations of phenanthrene and benzo(a)pyrene in the overlying water were monitored during the experiment. Fluxes were computed based on the sediment surface area of 120 cm² (8 cm wide by 15 cm long) and actual water flow rate of 4.5 mL/min. Results are shown in Figures 4.5 and 4.6. Fluxes were observed to progress from an initial value, increasing up to a certain maximum, and went down again. This trend may be reflective of the behavior of the organisms in that they would initially burrow into the sediment, stay there for a while without much activity. Then, after some days they would actively process the sediment until such time that they get relatively settled and stable. At this point, the worms still continue to actively process the sediment but in a calmer, more stable manner. Similar observations were obtained from tube experiments (data not shown) when worms were noticed to have actively processed the sediment during the third week. At that time, in some tubes, sediment was pushed up beyond the PVC ring fitted snugly in the tube to hold the cheese cloth placed on the surface of the sediment for feces collection. Some of the sediment was pushed up to rim of the tubes about 2-3 cm above the initial sediment level in the tubes.

Even during the highest activity of the worms, fluxes of phenanthrene and b[a]p are apparently small. As expected, concentrations of these PAHs in the overlying water were higher in worm microcosms than in the controls. The

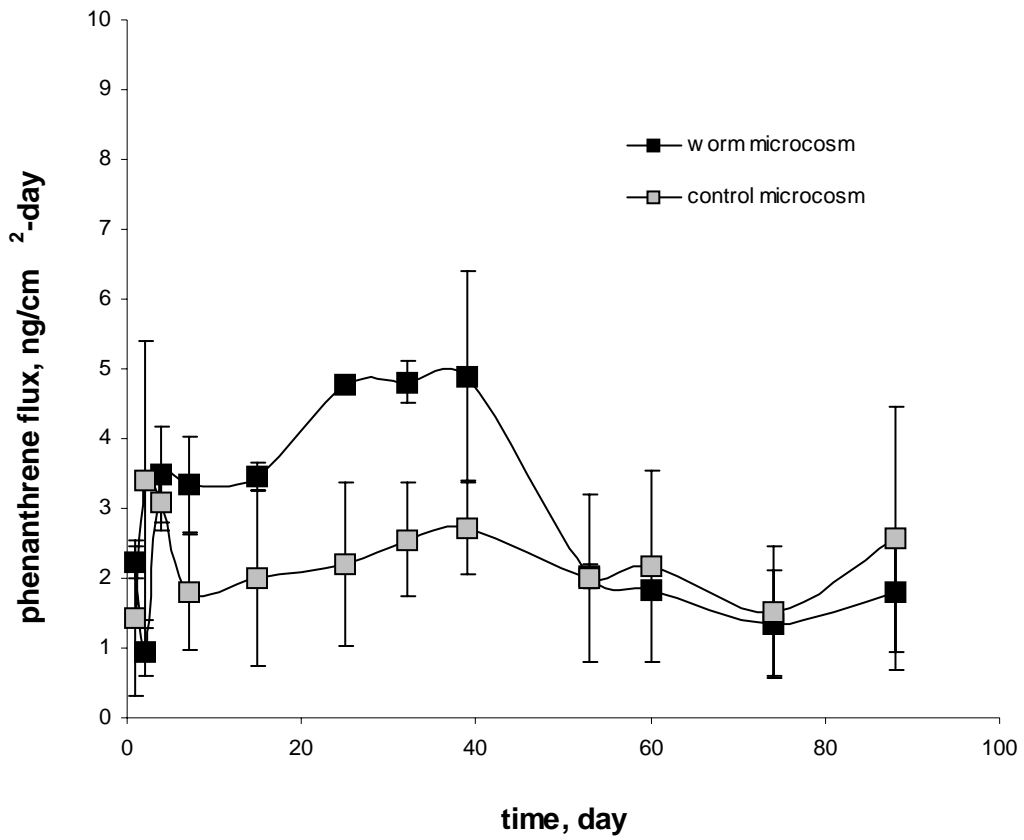


Figure 4.5. Flux of phenanthrene to overflow water in control and in worm microcosm. (means \pm std deviation, n=3 microcosms).

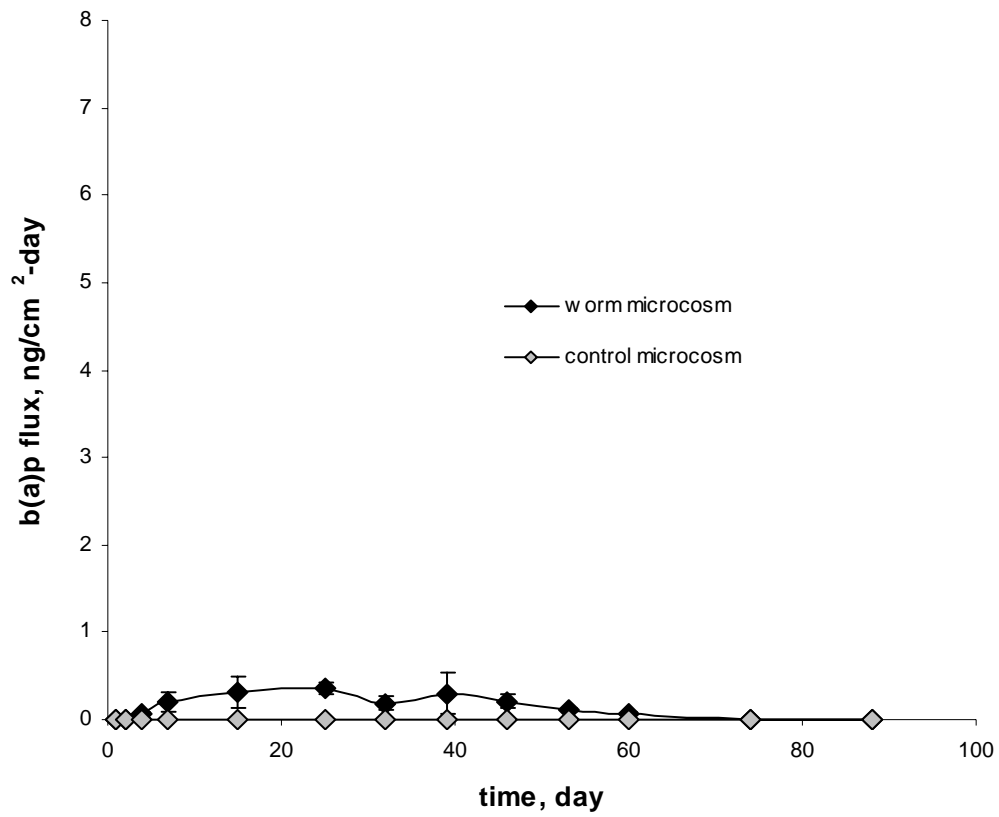


Figure 4.6. Flux of benzo(a)pyrene to overflow water in control and worm microcosm. (means \pm std deviation, n=3 microcosms).

differences however, were not of several orders of magnitude as reported of bioturbative fluxes compared to diffusive fluxes alone. This could be due to the desorption resistance of these PAHs as they may be bound strongly onto the sediment matrix. Our group in the laboratory had earlier determined that these PAHs in the Anacostia River sediment are primarily in the desorption-resistant fraction. Nevertheless, some small amounts of phenanthrene were detected in the water. Benzo(a)pyrene was detected only in the worm microcosms. With b[a]p, being desorption resistant, it is suggestive that transport of b[a]p to the overlying water would have occurred primarily by particle transport. Since overflow water samples were not filtered, b[a]p may have been directly extracted from entrained sediment in the water samples.

4.3.5 Concentrations of Phenanthrene and Benzo(a)Pyrene in the Sediment

4.3.5.1 Profiles of PAH Concentrations

Profiles of phenanthrene and benzo(a)pyrene concentrations at different sediment depths are shown in Figures 4.7 and 4.8, respectively.

The concentrations of phenanthrene at different depths in the control and worm-treated sediment showed profiles that overlap in the first 10-12 mm from the surface, then diverge up to about 62 mm below the surface, and converge again with high concentrations near the bottom. The curves may be divided into three parts: the part near the surface and the part near the bottom, both of which seem to have no significant difference between the control and the worm-treated sediment; and the part in the middle where it is assumed to be mostly affected by the activities of the

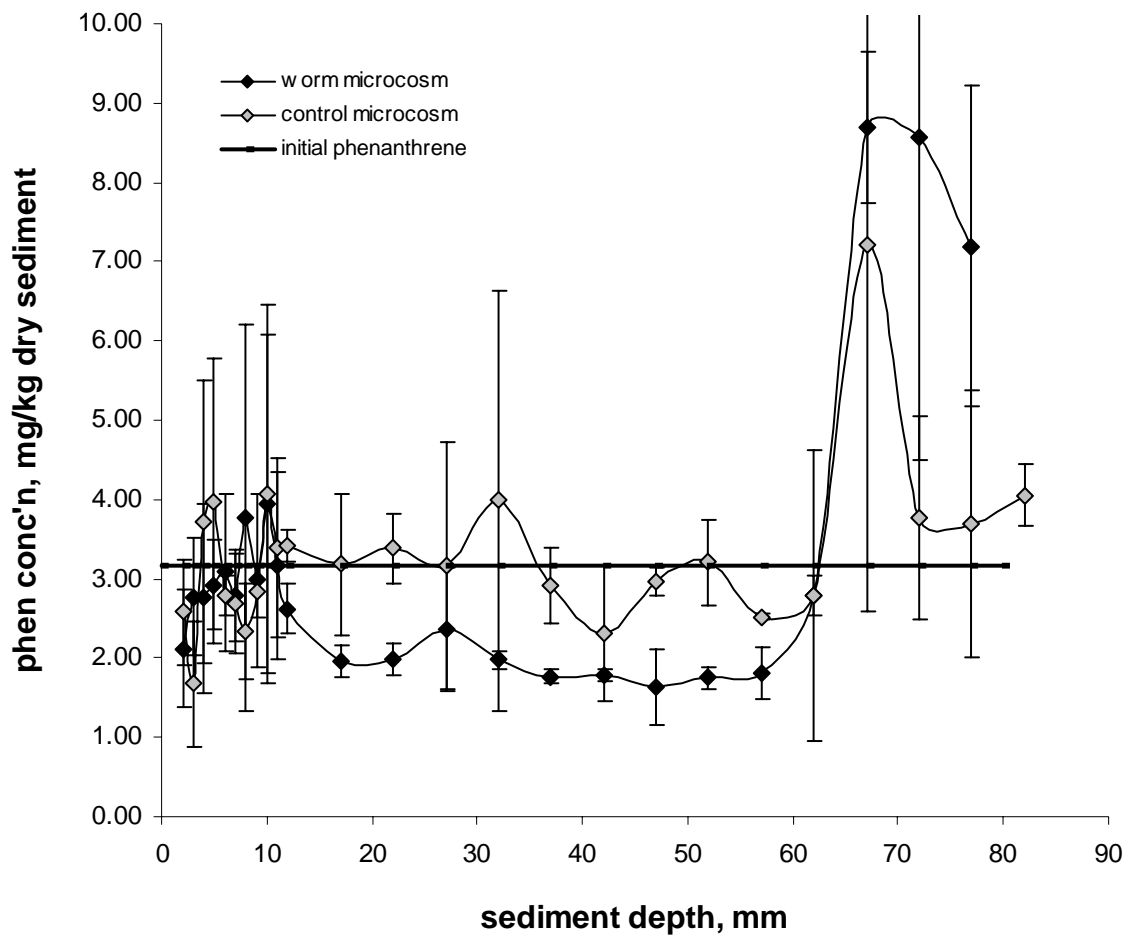


Figure 4.7 Profile of phenanthrene concentration in the sediment (means \pm std deviation, $n=2$ for the control microcosms, $n=3$ for the worm microcosms).

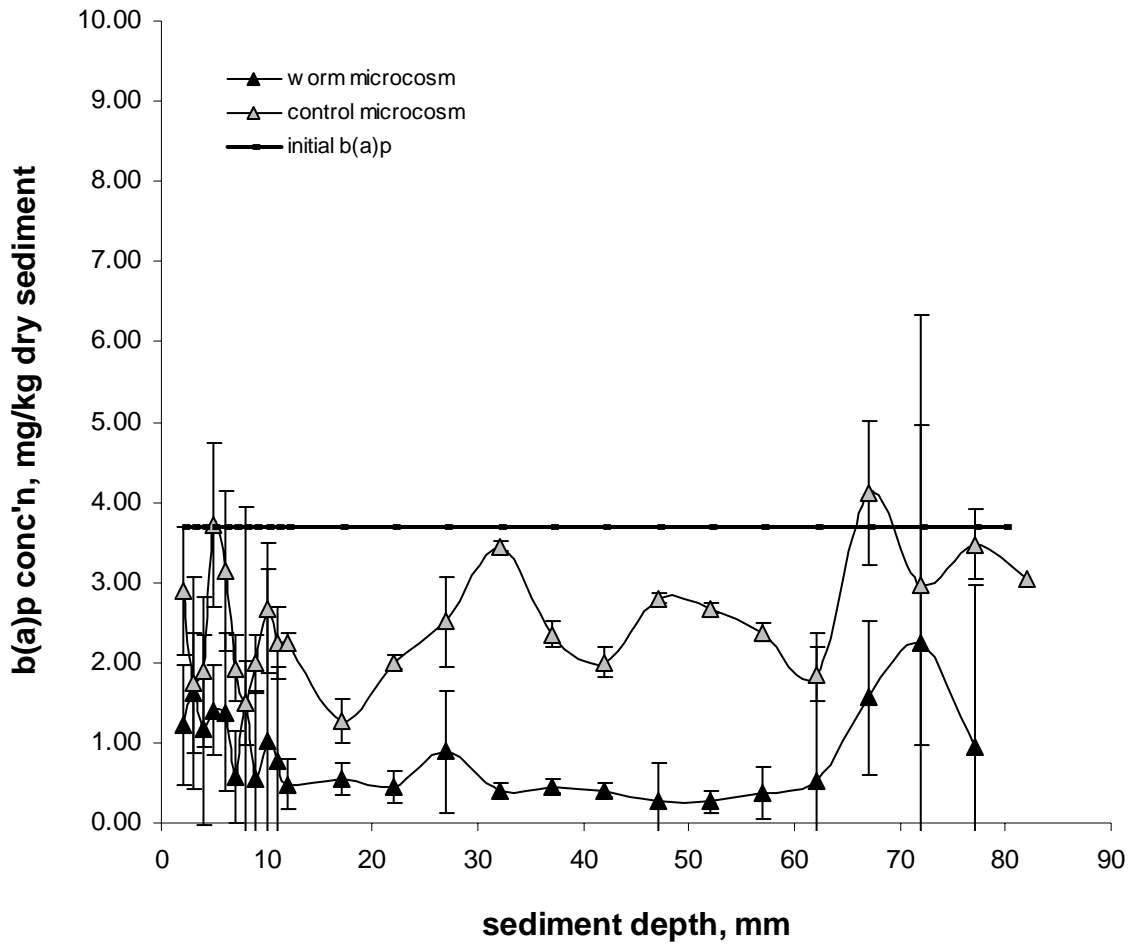


Figure 4.8 Profile of benzo(a)pyrene concentration in the sediment (means \pm std deviation, n=2 for the control microcosms, n=3 for the worm microcosms).

worms. It is in this middle part where by visual inspection of the curves, lower concentrations of phenanthrene were measured. What is quite intriguing in these results is the high and highly variable concentrations of phenanthrene observed below 62 mm from the sediment-water interface. These concentrations were even higher than the initial concentration of phenanthrene at the onset of the experiment. A similar trend was observed when preliminary sampling was done about a month after the initiation of the experiment (see Appendix A-1) to check the progress of the experiment. Profiles of phenanthrene also followed the same trend of increased concentration (albeit lower than what were observed during the final sampling) near the bottom. For the control, however, phenanthrene concentration profile was relatively constant at all depths during the preliminary sampling.

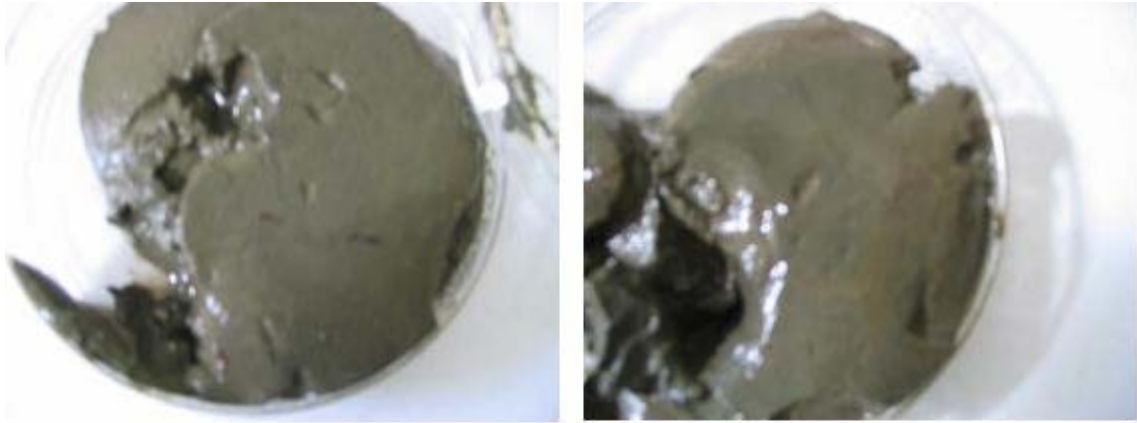
For the case of benzo(a)pyrene, a trend of increasing concentration near the bottom was also observed in both the control and worm microcosms. Again, preliminary determination of benzo(a)pyrene concentration profile (Appendix A-2) also showed similar trend, with higher concentrations observed near the bottom of the worm microcosm. Concentrations of b[a]p at most depths from the sediment surface are lower than the initial concentration for both microcosms.

Due to these earlier results, fractions of total organic carbon (TOC) of selected samples from different depths in the microcosms were analyzed. These TOC profiles for the control and the worm microcosm are shown in Appendix A-3. The TOC profile of sediment in the worm microcosm rose up beyond the 50mm depth, which coincides with the point at which phenanthrene in the worm microcosms also began

to increase in concentration beyond the initial value. A reasonable linear correlation between PAH concentration and organic carbon concentration was also observed (Appendix A-4 and Appendix A-5).

The results may suggest significant redistribution and transport of particles to the bottom of the microcosms. This transport is more pronounced in the worm microcosms. The activities of the worms may have facilitated transport of certain particles deeper into the sediment either through enhanced settling because of burrowing activities or probable selective worm processing of the sediment. Samples obtained from the bottom sections of the cells are described to have coarse and “chunky” consistency compared to samples obtained from the upper layers (see Figure 4.9 below). Unfortunately no particle size data are available to support this. The settled particles contain higher organic carbon in them. Hence, higher phenanthrene and benzo[a]pyrene concentrations were observed near the bottom as they are preferably partitioned to the organic carbon. These results may have implications not only on the organic matter preservation itself, but on the consequent transport and degradation of PAH as influenced by the oligochaetes.

The total phenanthrene and b[a]p recovered from the sediment at the end of experiment was determined from known concentrations and sediment weight of each of the sliced sediment. For both phenanthrene and benzo(a)pyrene, these are summarized in Table 4.3. All of the initial phenanthrene was recovered from the control while 90.22% (of initial amount) was recovered from the worm microcosms. It seems that any reductions of phenanthrene in the upper to the middle



(a)



(b)

Figure 4.9 Photos showing texture differences in sediment samples from the upper layers (a) and from the bottom (b).

Table 4.3. Total recovery of phenanthrene and benzo(a)pyrene from the control and worm microcosms.

	Total Recovery, % of Initial	
	Control Microcosm	Worm Microcosm
phenanthrene	116.75 ± 6.31	90.22 ± 6.52
benzo(a)pyrene	69.96 ± 11.13	21.40 ± 5.80

layers of the control microcosm were due only to redistribution to the bottom of higher-TOC-containing particles to which they are adsorbed. Concentrations of benzo(a)pyrene at most depths in the worm microcosm were significantly lower than those in the control. Overall, at the end of experiment, the total amounts of benzo(a)pyrene left in the control microcosms were higher than in the worm-treated sediment. Based on the table above, total reductions of 30.04 % and 78.60% were observed in the control and in the worm microcosms, respectively.

4.3.5.2 Mass Balances

For purposes of mass balances, the different routes for transport that determine the fate of phenanthrene and b[a]p in this study are assessed. The following are hereby considered:

- 1) bioaccumulation of the worms;
- 2) transport to the overlying water; and
- 3) degradation (biotic and/or abiotic)

Photodegradation and volatilization are some other possible routes. However these are neglected in the balances. Photodegradation can be assumed to be minimal because sediment samples for b[a]p extraction were taken from the center of each slice. Besides, as observed from the profiles, higher degradation occurred at some depths well below the surface where light penetration would not have been possible. In addition, any photodegradative effects may not be relevant in comparing the two cells (control and worm-treated) because no difference in photo-related factors were imposed.

The phenanthrene and benzo(a)pyrene concentrations determined in the worms at the end of the experiment are assumed to be the steady state tissue concentration, considering the 97-day length of exposure to the sediment. The concentrations are small in the case of this work, which was explained earlier to be probably due to high desorption-resistance of these PAHs in the sediment used. For 250 worms, these values are small and hence are a small fraction of the total PAH loss. Fluxes to the overlying water, as earlier noted, were also determined to be very small even in the presence of the worms. Summary of the results of the mass balances are given in Table 4.4 and Table 4.5.

The results suggest of some unaccounted phenanthrene and benzo(a)pyrene at the end of the experiment. Missing phenanthrene accounts for 20.47% of the amount initially present in the worm microcosm. Almost all of the phenanthrene in the control is accounted; losses are negligible. On the other hand, missing benzo(a)pyrene account for 81.57% and 29.93% of the initial amount present in the worm and control

microcosm, respectively. Considering all the different routes for the possible fate of these PAHs, the main factor, therefore, that may be considered responsible for the unaccounted phenanthrene and b[a]p is biodegradation. Biodegradation could either be due to microbial degradation or due to biotransformation by the worms themselves. Although no actual biotransformation study was done here, earlier work by Lu, et al. (2004) suggests that *I. templetoni* does not significantly biotransform benzo(a)pyrene. In their work, less than 6% of the parent b[a]p was metabolized during the 38-day exposure, and no strong trend over time was observed.

Table 4.4 Mass balances for phenanthrene in the control (C) and worm microcosms (W).

	Microcosm Cell				
	W1	W2	W3	C1	C2
Initial Total Weight,mg	2.00	2.05	2.06	1.93	1.98
Loss to bioaccumulation in worms, mg	0.0003	0.0003	0.0003	—	—
Loss due to flux, mg	0.035	0.033	0.032	0.018	0.026
Final total weight recovered, mg	1.46	1.73	1.66	1.91	2.11
“Missing” phenanthrene, mg	0.505	0.287	0.368	0.002	-0.156 (0)

(Number after microcosm name indicates replicate number).

Table 4.5 Mass balances for benzo(a)pyrene in the control (C) and worm microcosms (W).

	Microcosm Cell				
	W1	W2	W3	C1	C2
Initial Total Weight,mg	2.16	2.21	2.22	2.13	2.30
Loss to bioaccumulation in worms, mg	0	0	0	—	—
Loss due to flux, mg	0.002	0.001	0.001	0	0
Final total weight recovered, mg	0.41	0.62	0.38	1.30	1.66
Missing benzo(a)pyrene, mg	1.748	1.589	1.839	0.83	0.64

(Number after microcosm name indicates replicate number).

4.3.5.3. Enhanced Degradation of Phenanthrene and Benzo(a)Pyrene in Worm Microcosms

Enhanced degradation of phenanthrene and benzo(a)pyrene were suggested in worm microcosms. It is possible that the Anacostia River sediment used in the study may contain certain group or groups of microorganisms that are capable of biodegradation of phenanthrene and b[a]p, and are enhanced by the presence of the oligochaetes in the sediment.

The reduction of benzo(a)pyrene is unexpectedly high. Although phenanthrene is expected to be degraded more easily than b[a]p, the reverse is what was observed here. It has been observed in several experiments that the more aromatic rings there are in a compound, the less biodegradable it is. This is based on the premise that microbial uptake of the compound is initially through absorption from the aqueous phase. The more rings there are, the less soluble and less biodegradable a substance

is. Also, owing to the stability of the aromatic ring with respect to ring cleavage, more rings are more stable and would require more energy for cleavage and decomposition. The higher molecular weight PAH (greater than or equal to 4 rings) exhibited persistence that seemed to increase with the number of rings and the degree of ring condensation. However, these generalizations about structure-biodegradability relationship (SBR) in aerobic environments do not seem to be applicable to anaerobic environments (Alexander, 1999). Therefore, although it is generally reported that environmental persistence of polynuclear compounds increase with increasing number of rings, opposite trends have also been observed (De Weerd et al., 1986; Buisson et al., 1986; Genthner et al., 1989)

Another possible explanation for the higher degradation of b[a]p than phenanthrene could be the actual absence of phenanthrene degraders in the sediment. Many phenanthrene-utilizing isolates are *Pseudomonas* spp., *Sphingomonas* spp., or Gram positive bacteria of the *Nocardia*-*Rhodococcus*-*Mycobacterium* group, while the genera *Sphingomonas* and *Mycobacterium* seem to be specialized in degrading the less bioavailable compounds like benzo(a)pyrene (Wattiau, 2002).

Lastly, it may be important to address the issue of extraction efficiency of benzo(a)pyrene. Benzo(a)pyrene is a highly polar compound that may easily get intercepted by the presence of any fine particles entrained with the extract. This, combined with its low initial concentration in the sediment could have resulted to the low values observed.

Based on the profiles, it seems that the influence of the oligochaetes on the concentrations of phenanthrene and b[a]p occurs at some depths well below the surface. For b[a]p, this started from about 5 mm below the sediment-water interface. These results may seem to contradict the usual expectation that this influence should most likely occur at the surface of the sediment where oxygen penetration is possible, This relies on the common finding that PAHs are more easily biodegraded via the aerobic than the anaerobic pathway, as mentioned earlier. However, as each sediment is unique, so as the sediment used in the study.

4.4 Summary and Conclusions

The oligochaete *I. templetoni* was assessed to have significantly affected the physico-chemical characteristics of the sediment in microcosms. Lower concentrations of phenanthrene and benzo(a)pyrene were observed in worm microcosms. Concentration profiles of these PAHs show that these concentrations occurred well below the surface of the sediment. Mass balances done on the possible transport mechanisms suggest of biodegradation as the major fate pathway for phenanthrene and benzo(a)pyrene in this study.

Influence of the oligochaetes were observed on the following: dissolved oxygen in microcosms, redox potential of the sediment, and contaminant flux to the overlying water.

- With increased transport of oxygen from the overlying water in the presence of the oligochaetes, lower DO in the water was observed. This increased transport of oxygen may either be due to worm respiration and/or the effected enhanced oxygen demand of the sediment itself due to bioturbation.

- With respect to oxygen in the sediment, the results indicate the capability of the oligochaetes to increase penetration depth of oxygen in the sediment, in addition to increasing oxygen concentrations within this depth. Apparently, transport of oxygen into the sediment is limited by its diffusion through the pore water. Potential of bioturbation to overcome this however is possible.
- The worms were able to effectively change the redox profile of the sediment. This influence on sediment redox extends way below depths of DO penetration, and thus, may imply two things: a) The stimulation of redox potential in the sediment by the oligochaetes suggest that the stimulation pattern cannot be explained by the simple extension of the oxic layer; and hence, b) The use of the sediment redox potential over its DO may be a better and more dynamic parameter in assessing the influence of oligochaetes in the sediment.

CHAPTER 5

MICROBIAL ASSESMENT OF MICROCOSM SEDIMENTS BY DENATURING GRADIENT GEL ELECTROPHORESIS (DGGE): INITIAL MICROBIAL ANALYSIS

5.1 Introduction

As indicated in the previous chapter, one of the possible reasons for enhanced PAH degradation in the worm-inhabited microcosms is the enhanced biodegradation of phenanthrene and benzo(a)pyrene. Could the worms have actually affected the microbial population in the sediment in favor of enhanced biodegradation? If so, how may this had occurred and how may the microorganisms responded? In an effort to get an idea as to the impact of the oligochaetes on the microbial characteristics of the sediment, a DGGE analysis was done. This study may be the first to show how oligochaete pressure affected the microbial characteristics in the sediment using DGGE.

The results were expected to aid in explaining the increased degradation of phenanthrene and b[a]p as we attribute this to enhanced microbial population in the sediment due to the expected absence of abiotic fate mechanisms deep in the sediments. However, to fully understand the mechanisms involved in the interaction between the worms and the microorganisms with respect to the observed PAH degradation in this study, further efforts and experiments had to be done. Work done so far could serve as initial efforts in characterizing microbial populations as response factors to the presence of oligochaetes in PAH-contaminated sediments. The objectives of this molecular analysis work therefore are: 1) to assess the microbial

diversity as function of sediment depth in both the control and worm microcosms; and 2) to assess and compare microbial populations between control and worm microcosms using DGGE.

5.2 Denaturing Gradient Gel Electrophoresis as a Molecular Tool in Microbial Analysis

Molecular techniques based on nucleic acids have provided new insights into the diversity of microbial populations in the different ecological systems. The study of microbial communities has been greatly aided by the use of molecular methods allowing analysis of not only culturable, but also non-culturable microorganisms. This, in turn, provides us with the better understanding of relationships among ecosystem diversity, structure, and function.

The Denaturing Gradient Gel Electrophoresis (DGGE) is a molecular biological tool and technique, which is particularly helpful in studies that focus on changes in microbial assemblages as exposed to perturbation, or on how microbial composition changes with environmental gradients (e.g., depth in the water column, or in the sediment). One of the popular uses of DGGE has been in studies of microbial diversity and composition in the soil and sediment (Nakatsu, et al., 2000; Macnaughton, et al., 1999; Diez, et al., 2001; Muller, et al., 2002). These studies range from analysis of temporal and spatial variations of microbial populations, to diversity and functions of the populations exposed to certain perturbations or disturbances (e.g., introduction of contaminant to the soil or sediment).

On the other hand, DGGE is limited in its ability to indicate numerical dominance of certain populations in the sample. Quantitative analysis, based on the

presence and intensity of bands, to determine similarities between communities can also be subjective. This is especially the case when certain bands would appear very faint, and hence, the tendency to eliminate these bands for further analysis. This, on the other hand, could be due to limitations imposed by the resolution of the imaging system used. Other limitations may also be experienced in quantifying the extent of differences between communities of great diversity. Nevertheless, it is widely used as an initial tool, especially for samples with high microbial diversity.

5.3 Methodology

5.3.1 DNA Extraction

Frozen samples were thawed and vortexed for homogeneity prior to analysis. About 250-400 mg of sediment samples were extracted for DNA using Mo Bio UltraClean™ Soil DNA Isolation Kit (Mo Bio Laboratories, Inc., Solana Beach, CA), per the manufacturer's instructions, including the addition of 1.5 mL of 1x TE buffer and 0.02 g of polyvinyl polypyrrolidone (PVPP) to the sediment sample prior to the addition of the bead solution. This preliminary procedure was done to minimize on humic acids commonly present with soil samples that may interfere with the PCR.

Extracted DNA samples were then verified by visualization with UV light using standard agarose gel electrophoresis methods and staining with ethidium bromide. For until further analysis, nucleic acid extracts were stored at -20°C . A single DNA extraction was done for each depth of each microcosm, which was used in separate PCR reactions to produce products for multiple gel runs.

5.3.2 Polymerase Chain Reaction (PCR) Amplification

PCR amplification was performed in a Mastercycler (Eppendorf Scientific) using MasterTaq Kit (Eppendorf, Germany) and universal bacterial primers 341f (Casamayor et al., 2000) and 907r (Lane, 1991). The sequence of the 341f primer, which included a 40 base pair GC-clamp attached to the 5' end, was 5'-CGCCCGCCGCGCCCGCGCCCGTCCCGCCGCCCCGCCCCGCCTACGGGAGGCAGCAG-3', and the sequence of the 907r primer was 5'-CCGTCAATTCMTTTRAGTTT-3' (where M=C:A, R=A:G).

Amplification was done on a total volume of 50 μ L containing 1 μ L of the undiluted template DNA, 0.1-0.2 μ M of each of the primers, 0.2 mM of the deoxynucleoside triphosphate (dNTP) mix, 1.5 mM of Mg²⁺ (in Taq buffer), 2.5 units of the polymerase, 10 μ L of Taq enhancer, and sterile water to make up for the balance in volume. The PCR program initiates with initial denaturation of template DNA at 94°C for 5 minutes, followed by 30 cycles of the following steps: denaturation at 94°C for 1 minute, annealing at 53°C for 1 minute, and extension at 72°C for 1 minute. A single final extension was done at 72°C for 7 minutes. PCR products were refrigerated at 4°C until further analysis.

The sizing and quantification of DNA amplicons were done using the DNA 1000 Assays in conjunction with Agilent 2100 Bioanalyzer (Agilent Technologies) according to the manufacturer's protocol.

5.3.3 Denaturing Gradient Gel Electrophoresis

Separation of PCR-amplified 16S rDNA products by DGGE was performed using the BioRad DCode DGGE Apparatus. Each of the casted gels consisted of 24 mL polyacrylamide gel (6% w/v acrylamide) for 300-1000 base pair separation (D Code Universal Mutation Detection System Manual). The denaturant gradient ranges from 40% to 60% (where 100% denaturant contains 7M urea and 40% v/v formamide) and casting of the gel was accomplished using BioRad Model 475 Gradient Delivery System. Each gel was covered with 5 mL acrylamide stacking gel with no denaturant.

Electrophoresis was performed using the D-Code™ Universal Mutation Detection System (BioRad Laboratories, Hercules, CA) in 1 x TAE buffer (40mM Tris-acetate, 1 mM Na-EDTA) at 60°C and 65 volts for 15 hours. The gels were then stained with 25 µL of ethidium bromide solution in 1x TAE buffer for 10 minutes and washed twice in 1xTAE buffer and MilliQ H₂O prior to UV transillumination.

5.3.4 Analysis of DGGE Tracks

Scanned negatives after UV transillumination were analyzed using Quantity One 4.4 software (Bio-Rad, Hercules, Calif.). The software allows for band detection and matching in and among the lanes in the gel. The lanes were initially framed manually and pixel intensity profile for each lane was generated with background subtraction at a rolling disk size of 5. Automatic detection of the bands were done at sensitivity of 10, at maximum shoulder sensitivity, with normalization due to differences in lane intensity, and with rejection of shadows which are common

artifacts in gels. Detected bands were further screened by rejecting bands with relative quantity of less than 1%. Automatic matching of bands was then done at 1% level of tolerance.

Comparisons between samples by comparisons of the lanes on the gel were made based on the presence or absence of bands. Bands from two different lanes are considered identical if they have traveled the same distance on the gel. Each sample was scored based on the presence or absence of each band in its profile when compared to the profile of each of the other samples.

5.3.5 Quantitative Analysis of DGGE Fingerprints

Similarity coefficients for pair wise comparisons of lanes on the DGGE gels were calculated using the non-weighted Dice's similarity coefficient (C_s). Based on the presence or absence of bands, the Dice's coefficients were computed as follows (La Para, et al., 2002):

$$C_s = 100 \times 2j / (a + b)$$

where a and b are the number of bands in lane A and lane B, respectively, while j is the number of bands common to both lanes. This coefficient ranges from a value of 0 (no common bands) to 100 (all bands are common).

5.4 Results and Discussions

Successful DNA extraction was performed from the sediment matrix samples. PCR amplifications of these extracts were also successful as verified by agarose gel electrophoresis. Further analysis by sizing and quantification of DNA amplicons, however, indicate low concentrations of the target DNA (640 bp in length).

Nevertheless, these were loaded in the DGGE gel with the dye in equal volume to maximize the total volume of sample that the wells can hold. A 40-60% denaturant gradient was used, based on earlier results with 40-70% gel (data not shown), which showed clustering of multiple bands within approximately the 50-60% denaturant. Therefore, to get better resolution and identification of bands in the cluster, a 40-60% gradient was used.

Shown in the following are microbial profiles of selected samples obtained from different depths in the sediment determined by the molecular technique of denaturing gradient gel electrophoresis. Each of the lanes on the gels represents microbial profiles of samples obtained from a particular depth in the microcosm. These depths in the microcosm were arbitrarily chosen representative of three zones along the sediment column (Table 5.1) based on the observed profiles of phenathrene and benzo(a)pyrene concentrations in the sediment. These zones are: the upper zone, which ranges from the surface to about 6mm in the sediment; the middle zone; and

Table 5.1 Depth description of samples obtained from different zones in the microcosms.

Zone	Depths from the sediment surface where samples were obtained
Upper Zone	2 mm, 4 mm, 6 mm
Middle Zone	12 mm, 22 mm, 52 mm
Bottom Zone	62 mm, 72 mm

the bottom zone, which was least likely processed by the worms. The bottom zone is characterized by coarser and relatively larger particles as earlier described. There were a total of eight samples from each sliced microcosm analyzed by DGGE.

In Figure 5.1 shown are profiles of samples taken from two replicate worm cells (Note: Bands were identified only by visual inspection for purposes of this discussion. More bands were automatically detected as will be shown in later discussions comparing worm-treated with control microcosm.). Apparently, these cells have similar microbial profiles, which vary with depth from the sediment surface. Trends in the appearance and disappearance of bands along the different depths of the sediment are similar for both replicates. For instance, bands 1,2,3, and 4 tend to appear only in the upper 2-6 mm (lanes 1 to 3, and lanes 9 to 11) of the sediment of both microcosms, suggesting that these are aerobic microorganisms, which would thrive only in the upper oxic layer. Another suggestion is that these bands represent some groups of aerobic microorganisms grazed upon by the worms and that they begin to fade way down into the sediment, probably in those layers within reach of the worms as they burrow head down into the sediment. Near the bottom of the gel, the lanes are characterized by a cluster of about six to eight bands all together. Some of these bands, i.e., bands 13 and 15, begin to disappear at the bottom zone. The bottom zones (lanes 7-8 and lanes 15-16) are characterized by the appearance of the least number of bands.

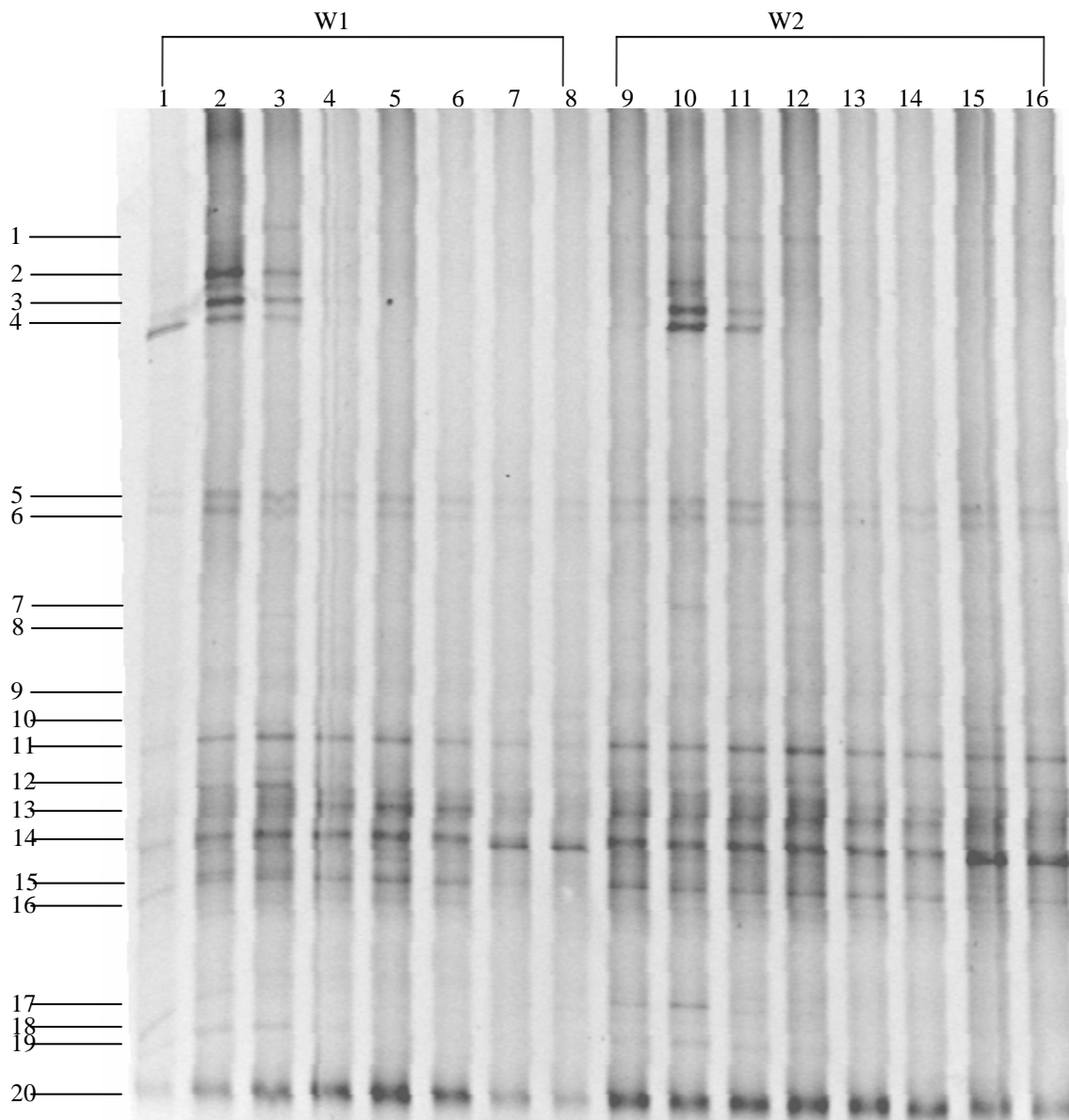


Figure 5.1 Negative image of DGGE gel (40-60% denaturant) comparing samples from two replicate worm (W) microcosms: W1 (lanes 1-8); W2 (lanes 9-16).

(Note: Bands were identified only by visual inspection for purposes of discussion.)

Lane #	Depth from Sediment Surface, mm
1 and 9	2
2 and 10	4
3 and 11	6
4 and 12	12
5 and 13	22
6 and 14	52
7 and 15	62
8 and 16	72

Figure 5.2 shows representative samples from different depths in two control microcosms. At a given depth in the control sediment, profiles of bands look similar except for those of the first 4 lanes of the two replicates. It is on these lanes where the more number of bands was observed. Most of the differences occurred on the upper part of the gel where control microcosm #2 (C2) showed some bands that are not present in control microcosm #1 (C1). If the first four bands earlier identified with the first three lanes of the worm microcosms are the same bands also present in the first three lanes of the control, this may discount the possibility of worm grazing as an explanation for their disappearance beyond the first three lanes. Midway on the gel, a band identified from the figure as band #20 consistently appeared at all depths in the control microcosms while bands 21, 23, and 24 begin to fade away beyond the first three lanes of the controls.

To compare the microbial profiles between the control and worm microcosms , samples from one of the worm cells and samples from one of the control cells were loaded in the same gel. Since samples were taken from two worm cells and two control cells, two gels were prepared for this purpose and DGGE profiles are shown in Figure 5.3 and Figure 5.4. These profiles also show a middle lane (lane #9), which represents sample obtained from the original sediment at the onset of the experiment. It is difficult to compare between gels due to the biases of the DGGE technique and the fact that no marker was used in the analysis. Therefore comparisons between the treatment effects were done only between lanes on the same gel.

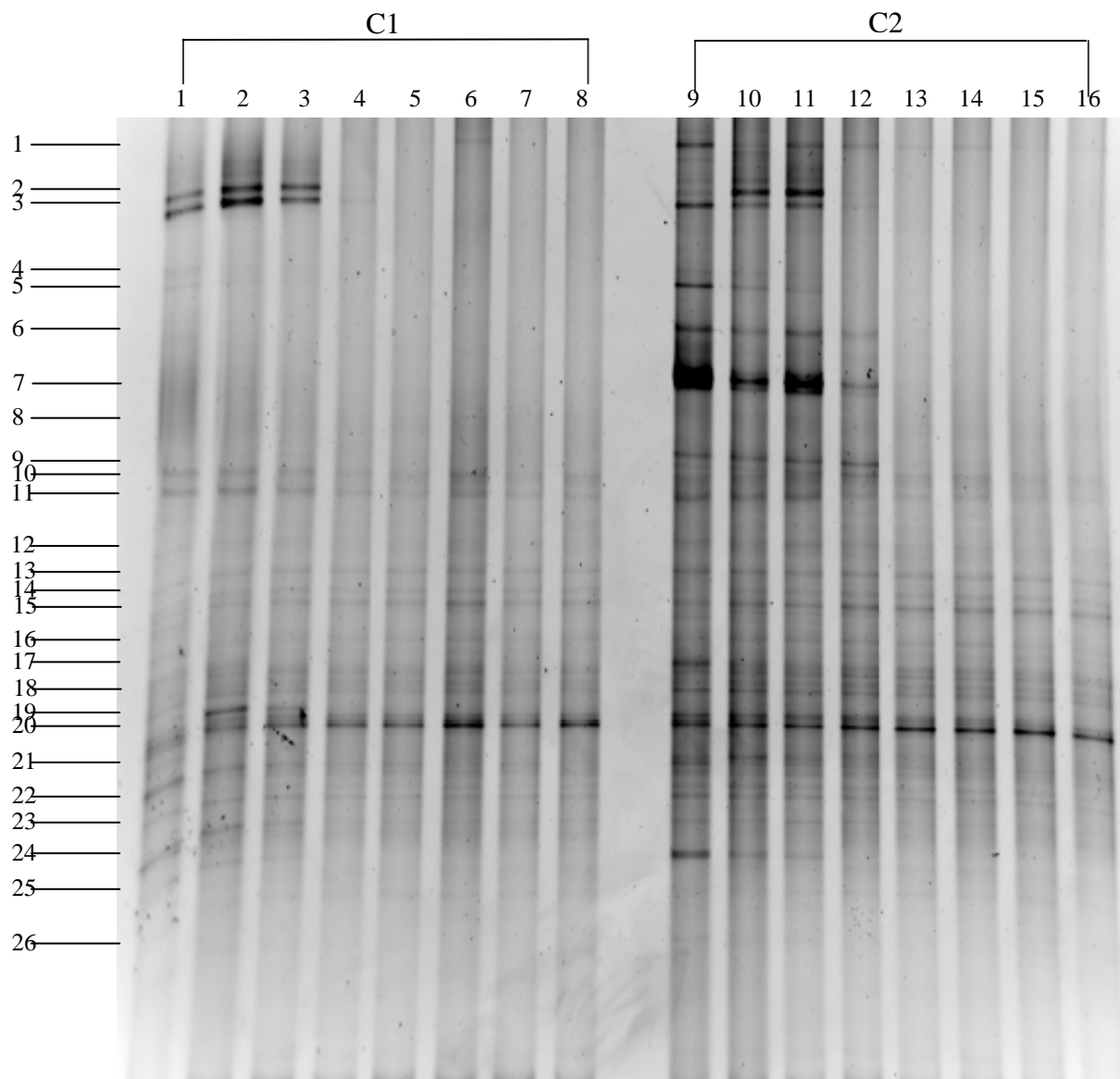


Figure 5.2 Negative image of DGGE gel (40-60% denaturant) comparing samples from two replicate control (C) microcosms: C1 (lanes 1-8); C2 (lanes 9-16).

(Note: Bands were identified only by visual inspection for purposes of discussion.)

<u>Lane #</u>	<u>Depth from Sediment Surface, mm</u>
1 and 9	2
2 and 10	4
3 and 11	6
4 and 12	12
5 and 13	22
6 and 14	52
7 and 15	62
8 and 16	72



Figure 5.3. Negative image of DGGE gel (40-60% denaturant) comparing samples from worm microcosm 1 (W1) and control microcosm 1 (C1). Original sediment (lane 9) is also shown for further comparisons.

<u>Lane #</u>	<u>Depth from Sediment Surface, mm</u>
1 and 10	2
2 and 11	4
3 and 12	6
4 and 13	12
5 and 14	22
6 and 15	52
7 and 16	62
8 and 17	72

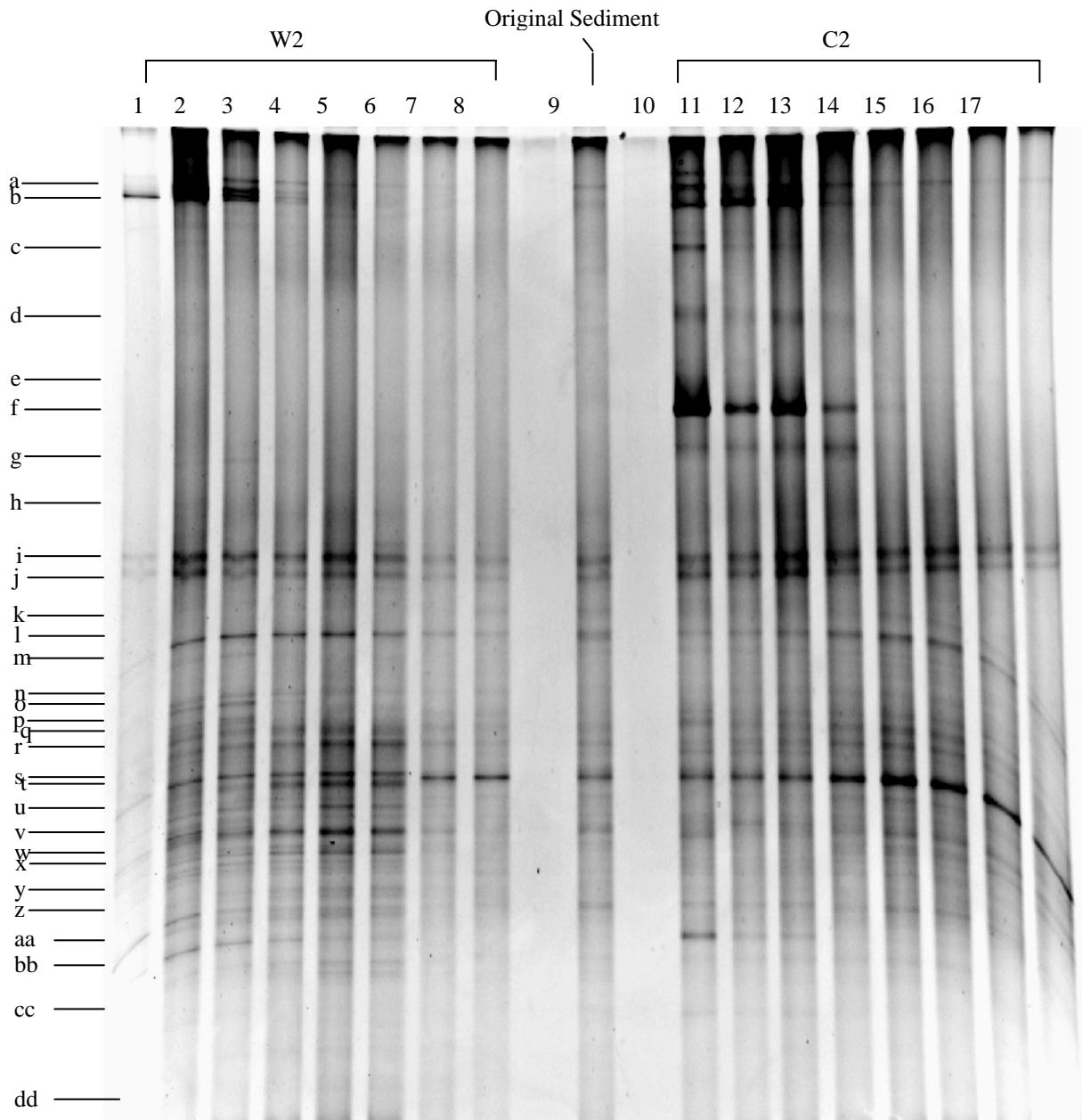


Figure 5.4. Negative image of DGGE gel (40-60% denaturant) comparing samples from worm microcosm 2 (W2) and control microcosm 2 (C2). Original sediment (lane 9) is also shown for further comparisons.

<u>Lane #</u>	<u>Depth from Sediment Surface, mm</u>
1 and 0	2
2 and 11	4
3 and 12	6
4 and 13	12
5 and 14	22
6 and 15	52
7 and 16	62
8 and 17	72

Comparison of profiles between worm microcosm #1 (W1) and control microcosm #1 (C1) suggests some differences between the two treatments (see Figure 5.3). Some of these differences occur in the upper gel of the first three lanes where certain bands appear very faintly in the first three lanes of the worm microcosm compared to those in the control. Within the cluster of bands near the bottom of the gel, band u tends to show up as an intense, distinct band at all depths in C1, the last two lanes of W2, as well as in the original sediment sample (lane 9). Certain bands (x, y, and cc) tend to appear dominant in W1 than in corresponding lanes of C1.

Comparison of profiles between the worm microcosm #2 (W2) and control microcosm #2 (C2), also show differences in the upper part of the gel for the first three lanes of each microcosm (see Figure 5.4). Again in the middle zone, certain bands (i.e., bands t, u, v, and w) tend to appear only in the worm microcosm but not in the corresponding region of the control microcosm.

Quantitatively, comparison of the control and the treated microcosms was done using the Dice coefficient values calculated from comparison of profiles obtained at the same depth of each of the microcosms. These are summarized in Table 5.2. The Dice coefficient values generally show considerably low index of similarity between the worm and control microcosm. On the average, based on the depth-per-depth comparison, W₁-C₁ comparison has a Dice index of 59.6, while W₂-C₂ comparison has 52.9. Indeed, there is considerable difference in the microbial profiles of the worm and the control microcosms.

Table 5.2. Dice index coefficients for comparison of control and worm microcosm.

Depth, mm	Compared Lanes	W₁ vs C₁	W₂ vs C₂
2	lane 1 vs lane 10	48.1	55.8
4	lane 2 vs lane 11	63.6	54.4
6	lane 3 vs lane 12	58.4	54.3
12	lane 4 vs lane 13	58.2	51.2
22	lane 5 vs lane 14	57.1	59.3
52	lane 6 vs lane 15	55.2	49.7
62	lane 7 vs lane 16	71.4	49.3
72	lane 8 vs lane 17	64.8	49.5
	Average	59.6	52.9

These differences are primarily due to the presence or absence of bands in the upper zone and the middle zone. The bottom zones of the two treatments tend to look similar. The middle zone corresponds approximately to the region of worm processing as they burrow head down to the sediment, it may be suggestive that the bands which appear only in the middle zone of the worm microcosm, represent some groups of microorganisms that are probably enhanced either directly or indirectly by the presence of the worms. It is possible that these groups may live in some co-metabolic or mutualistic activities with the each other. Therefore, even if only some of these bacteria may be directly affected by the worms, the others could be enhanced by the presence of these groups. Hence, they would also appear to be present with relatively higher intensity in the middle zone of the worm microcosms.

Lower molecular-weight PAHs, like phenanthrene, are readily degraded by a number of aerobic bacteria which can utilize them as sole carbon and/or energy

source. On the other hand, higher molecular-weight PAHs, like benzo(a)pyrene are co-metabolically degraded by only a few bacterial species like *Mycobacterium* spp. and *Sphingomonas* spp. (Steffen, et al., 2003).

5.5 Conclusions

Successful DNA extraction and separation of PCR-amplified 16S rDNA products using DGGE as a means to describe diversity of microbial community in PAH-contaminated sediment were accomplished. The large number of bands determined at different depths of the worm and control microcosms indicate species richness in both microcosms.

Banding patterns observed at different depths differ, which clearly indicate the dependency of the banding pattern on the microcosm depth. Microbial diversity varies at different depths in the microcosms, which may imply microbial distribution as a function of oxygen concentration in the sediment. The non-weighted Dice indices of similarity computed for comparisons of the worm and control sediment sampled at the same depth in the microcosms also indicate considerably dissimilar microbial profiles. This suggests significant influence of the worms on the microbial population in the sediment. Apparently, there existed an interaction between the worms and the indigenous microbes in the sediment. The nature of this interaction could not be clearly defined at this time as microbial functions may not be concluded from DGGE profiles. However, it is suggested that there appeared to be some bands representative of some groups of microorganisms that are either directly or indirectly enhanced by the presence of worms in the microcosm. The latter would mean that some groups

that are directly enhanced by the worms can enhance another group of microorganisms not necessarily affected by the worms.

DGGE analysis has proven to be an important tool for comparison between samples. It can be a powerful tool for initial microbial analysis to discriminate communities and to determine numerically dominant bands. However, no conclusion could be drawn as to microbial functions that could relate to the degradation of phenanthrene and benzo(a)pyrene in worm microcosms.

CHAPTER 6

CONCLUSIONS AND RECOMMENDATIONS

6.1 Conclusions

The oligochaete *I. templetoni* was assessed to have significantly affected the physico-chemical characteristics, as well as the microbial characteristics of the sediment in microcosms. Influence of the oligochaetes was observed on the following: dissolved oxygen in microcosms, redox potential of the sediment, contaminant flux to the overlying water, and sediment microbial diversity.

- With increased transport of oxygen from the overlying water to the sediment, lower water DO was observed in worm microcosms. This increased transport of oxygen to the sediment may either be due to worm respiration and/or the effected enhanced oxygen demand of the sediment itself due to bioturbation.
- With respect to oxygen in the sediment, the results indicate the capability of the oligochaetes to increase penetration depth of oxygen in the sediment, in addition to increasing oxygen concentrations within this depth. Apparently, transport of oxygen into the sediment is limited by its diffusion through the pore water. Potential of bioturbation to overcome this however is possible.
- The worms were able to effectively change the redox profile of the sediment. This influence on sediment redox extends way below depths of DO penetration. This may imply two things: a) The stimulation of redox potential in the sediment by the oligochaetes suggest that the stimulation pattern cannot be explained by simple extension of the oxic layer; and hence b) The use of

redox potential over DO may be a better and more dynamic parameter in assessing the influence of oligochaetes in the sediment.

- The flux of sediment phenanthrene and benzo(a)pyrene was higher in worm microcosms. However, these values are small probably due to the desorption-resistance of the PAHs in the sediment. The higher hydrophobicity of benzo(a)pyrene rendered it undetectable in the overlying water of the control microcosms.
- Successful DNA extraction and separation of PCR-amplified 16S rDNA products using DGGE as a means to describe diversity of microbial community in PAH-contaminated sediment were accomplished. DGGE profiles obtained indicate high species richness in the microcosms. Microbial diversity also varied with different depths in the same microcosm. Dice indices of similarity determined from the worm and control sediments sampled from the same depth in the microcosms also indicate considerably different microbial profiles. There may have existed an interaction between the worms and the indigenous microbes in the sediment. The nature of this interaction could not be clearly defined at this time as microbial functions may not be concluded from DGGE profiles. However, it is suggested that there appeared to be some bands representative of some groups of microorganisms that are either directly or indirectly enhanced by the worms.

Enhanced degradations of phenanthrene and benzo(a)pyrene were observed in worm-inhabited microcosms. Concentration profiles of these PAHs show that the

lowest concentrations occurred well below the surface of the sediment. Mass balances done reveal some “missing” phenanthrene and benzo(a)pyrene from the microcosms. After consideration of the different possible transport mechanisms for the PAHs, it is strongly suggested that biodegradation is the major fate pathway for phenanthrene and benzo(a)pyrene in this study.

Biodegradation of phenanthrene, but more especially of benzo(a)pyrene, was enhanced by the presence of the oligochaete in the microcosms. There are two issues here that need to be addressed though – 1) Does the mechanism involve an enhanced aerobic or anaerobic microbial biodegradation?, and 2) What may be the mechanism of direct influence on the microbial community by the oligochaetes?

Results (i.e., low concentration profiles well below the sediment surface, and way beyond penetration depth of oxygen) may suggest that an enhanced anoxic/anaerobic degradation occurred. However, the possibility of aerobic degradation may not be totally discounted. This is because it may have been possible that pulses of oxygen were supplied in the lower layers due to the activities of the worms. These, however, could have been used up immediately by microbial processes. As such, they were not detected beyond the apparent DO penetration depth observed here.

Direct enhancement of microbial degraders by the oligochaetes may have also occurred, possibly due to certain mucus secretions, or direct pressure on certain groups of microorganisms. However, no data to support this are available in this work.

6.2 Recommendations

To improve our understanding and analysis of the results herein obtained the following are some recommendations that may need further considerations:

- Results on the physico-chemical influence of the oligochaetes with respect to biodegradation suggest merit for further studies on understanding the dynamics of redox potential and oxygen transport in the sediment. For instance, changes of dissolved chemical species along with oligochaete-influenced Eh may need to be determined.
- Benthos-mediated particle transport (particle settling, in particular) within the sediment columns may also have some implications on the assessment of contaminant degradation, which may vary with depth in the sediment. Hence is also an exciting area of further research.
- The possible occurrence of anoxic to anaerobic degradation of phenanthrene and b[a]p was suggested in the results of this study. Careful investigation of the results, however, indicate the need for further analysis and determination of microbial activity in the sediment that would actually reflect microbial functions that could be directly related to the observed degradation. Certain bands on the DGGE gel which appeared to have been enhanced by the oligochaetes may merit identification. This is expected to aid in elucidating the interaction that exists between *I. templetoni* and the sediment microorganisms with respect to their role on the observed phenanthrene and benzo(a)pyrene degradation.

This study assumes negligible transformation of the PAHs by *I. templetoni* based on results obtained by Lu (2004). However, for the case of long experiments, would it not be possible that *I. templetoni* will be able to transform the PAHs? If so, would the biotransformed PAHs be more available for microbial attack? Biotransformation experiment is hereby suggested to determine the potential of the oligochaetes to biotransform b[a]p, and to be able to identify these biotransformed products. It may also be necessary to determine whether these biotransformed products are more biodegradable to the microorganisms. Hence, a biodegradation experiment using the parent compound and biotransformed products as substrates may be done.

REFERENCES

Alexander, M. 1999. *Biodegradation and Bioremediation*. 2nd ed. Academic Press, New York, USA.

Aller R.C. 1982. The effects of macrobenthos on chemical properties of marine sediment and overlying water. In: McCall P.L., Tevesz M.J.S., editors. *Animal-Sediment Relations*. New York, Plenum Press.

Aller R.C. 1994. Bioturbation and remineralization of sedimentary organic matter: Effects of redox oscillation. *Chemical Geology*, 114, 331-345.

American Society for Testing and Materials. 1998. Standard test method for determining a sorption constant (*K_{oc}*) for an organic chemical in soil and sediment. E 1195-87. In *Annual Book of ASTM Standards*, Vol 11.02. Philadelphia, PA, USA, 731-737.

American Society for Testing and Materials. 1997. Standard guide of the bioaccumulation of sediment-associated contaminants by benthic invertebrates. E 1688-97a. In *Annual Book of ASTM Standards*, Vol 11.05. Philadelphia, PA, USA, 1075-1124.

Beck, T.C. 1972 Daily patterns of oxygen consumption in *Limnodrilus hoffmeisteri*. *M.S. Thesis*. Western Michigan University. 76 pp.

Berry, D.F., A.J. Francis, and J.M. Bollag. 1987. Microbial Metabolism of Homocyclic and Heterocyclic Aromatic Compounds Under Anaerobic Conditions. *Microbiology Reviews*, 51, 43-59.

Bosma TNP, Middeldorp PJM, Schraa G, Zender AJB .1997. Mass transfer limitation of biotransformation: quantifying bioavailability. *Environ Sci Technol*. 31, 248–252.

Brinkhurst R.O., Cook D.G. 1980. *Aquatic Oligochaete Biology*. Plenum Press, New York, NY.

van de Bund, W.J., Goedkoop, W., and Johnson, R.K. 1994. Effects of deposit-feeder activity on bacterial production and abundance in profundal lake sediment. *Journal of the North American Benthological Society*, 13, 532-539.

Casamayor, EO, Schafer, H, Muyzer, G. 2000. Identification of spatio-temporal differences between microbial assemblages from two neighboring sulfurous lakes: comparison by microscopy and denaturing gradient gel electrophoresis. *Applied and Environmental Microbiology*, 66, 499-508.

Cerniglia CE, Heitkamp MA (1989) Microbial metabolism of polycyclic aromatic hydrocarbons (PAH) in the aquatic environment. In: Varanasi U (ed) *Metabolism of Polycyclic Aromatic Hydrocarbons in the Aquatic Environment*. CRC, Boca Raton, Fla, pp 41–68.

Coates, J.D., R.T. Anderson, J.C. Woodward, E.J.P. Phillips, and D.R. Lovley. 1996. Anaerobic hydrocarbon degradation in petroleum-contaminated harbor sediments under sulfate-reducing and artificially imposed iron-reducing conditions. *Environmental Science and Technology*, 30, 2784-2789.

Coates, J.D., J. Woodward, J. Allen, P. Philip, and D.R. Lovley. 1997. Anaerobic degradation of polycyclic aromatic hydrocarbons and alkanes in petroleum-contaminated marine harbor sediments. *Applied and Environmental Microbiology*, 63, 3589-3593.

Cunningham, P.B. 2002. Influence of tubificid oligochaetes on the fate of pyrene in contaminated sediment. *Ph.D. Dissertation*, Louisiana State University, Baton Rouge, LA., USA. (In review).

Diez, B., Pedros-Alio, C., Marsh, T.L. and R. Massana. 2001. Application of denaturing gradient gel electrophoresis (DGGE) to study the diversity of marine picoeukaryotic assemblages and comparison of DGGE with other molecular techniques. *Applied and Environmental Microbiology*, 67, 2942-2951.

Driscoll, S. K., McElroy, A. E. 1996. Bioaccumulation and metabolism of benzo[a]pyrene in three species of polychaete worms. *Environmental Toxicology and Chemistry*, 15,1401-1410.

Evans, W. C. 1988. Anaerobic degradation of aromatic compounds. *Annual Review of Microbiology*, 42, 289-317.

Fasnacht, M.P. and N.V. Blough. 2002. Aqueous photodegradation of polycyclic aromatic hydrocarbons. *Environmental Science and Technology*, 36, 4364-4369.

Fenchel T. 1996. Worm burrows and oxic microniches in marine sediments. 1. Spatial and temporal scales. *Marine Biology* , 127, 289-295.

Forster, S. and G. Graf. 1992. Continuously measured changes in redox potential influenced by oxygen penetrating from burrows of *Callianassa subterranea*. *Hydrobiologia*, 235/236, 527-532.

Giessing AM, Mayer LM, Forbes TL. 2003. 1-Hydroxypyrene glucuronide as the major aqueous pyrene metabolite in tissue and gut fluid from the marine deposit-feeding polychaete *Nereis diversicolor*. *Environ Toxicol Chem.* , 22, 1107-14.

Gert-jan De Maagd, P. *et al.* 1998. Physical properties of polycyclic aromatic hydrocarbons: aqueous solubilities, *n*-octanol/water partition coefficient, and Henry's law constants. *Environmental Toxicology and Chemistry*, 17, 251-257.

Hambrick III, G. A., DeLaune, R. D., and W. H. Patrick, Jr. 1980. Effect of estuarine sediment pH and oxidation-reduction potential on microbial hydrocarbon degradation. *Applied and Environmental Microbiology*, 40, 365-369.

Hansen, K. and Kristensen, E. 1997. Impact of macrofaunal recolonization on benthic metabolism and nutrient fluxes in a shallow marine sediment previously overgrown with macroalgal mats. *Estuarine Coastal and Shelf Science*, 45, pp 613-628.

Harms H, Bosma TNP. 1997. Mass transfer limitation of microbial growth and pollutant degradation. *J Ind Microbiology*, 18, 97-105.

Hemond, H.F., and E.J. Fechner. 1994. *Chemical Fate and Transport in the Environment*. Academic Press, New York, U.S.A., pp. 97-107.

Herbes, S., (1977) Partitioning of polycyclic aromatic hydrocarbons between dissolved and particulate phases in natural waters. *Water Research*, 11, 493-496.

Herbes SE, Schwall LR. 1978. Microbial transformation of polycyclic aromatic hydrocarbons in pristine and petroleum-contaminated sediments. *Applied Environmental Microbiology*, 35, pp 306-316.

Holmer, M., Forbes, V.E., and T.L. Forbes. 1997. Impact of the polychaete *Capitella* sp. I on microbial activity in an organic-rich marine sediment contaminated with the polycyclic aromatic hydrocarbon fluoranthene. *Marine Biology*, 128, 679-688.

Kadlubar, F. F. & Hammons, G. J. (1987) The role of cytochrome P-450 in the metabolism of chemical carcinogens. In Guengrich, F. P. (ed.), *Mammalian Cytochromes P-450*. Vol. II . CRC Press, Boca Raton, FL: 81-130.

Kanaly, R.A., and S. Harayama. 2000. Biodegradation of high-molecular-weight hydrocarbons by bacteria. *Journal of Bacteriology*. 182: 2059-2067.

Kristensen, E. 2000. Organic matter diagenesis at the oxic/anoxic interface in coastal marine sediments, with emphasis on the role of burrowing animals. *Hydrobiologia*, 426, 1 – 24.

Kristensen, E. 1988. Benthic fauna and biogeochemical processes in marine sediments: microbial activities and fluxes. In Black- burn, T. H. & J. Sørensen (eds), *Nitrogen Cycling in Coastal Marine Environments*. John Wiley & Sons Ltd., Chichester: 275-299.

- Lane, D.J. 1991. 16S/23S rRNA sequencing. In: Stackbrandt, E., Goodfellow, M. (eds) *Nucleic Acid Techniques in Bacterial Systematics*. John Wiley, Chichester, UK, pp 115-175.
- LaPara T.M., Nakatsu, C.H., Pantea, L.M. 2002. Stability of the bacterial communities supported by a seven-stage biological process treating pharmaceutical wastewater as revealed by PCR-DGGE. *Water Research*, 36, 638–646.
- Lotufo, G.R., 1998. Bioaccumulation of sediment-associated fluoranthene in benthic copepods: Uptake, elimination and biotransformation. *Aquatic Toxicology*, 44,1-15.
- Lu, X.X., Reible D.D., Fleeger J.W., Chai, Y.Z. 2003. Bioavailability of desorption – resistant phenanthrene to Oligochaete, *Ilyodrilus templetoni*. *Environmental Toxicology and Chemistry*, 22,153-160.
- Lu, X.X., Reible, D.D., Fleeger, J.W., Bioavailability, and assimilation of sediment-associated benzo[a]pyrene by *Ilyodrilus templetoni* (Oligochaeta). *Environmental Toxicology and Chemistry*, 23, 57-64.
- Lu, X.X., Reible, D.D., Fleeger, J.W. 2004. Bioavailability and assimilation of sediment-associated benzo(a)pyrene by *Ilyodrilus templetoni* (Oligochaeta). *Environmental Toxicology and Chemistry*, 23, 57-64.
- Maranto, L. 1996. Bioturbation enhanced contaminant release from bed sediments. *M.Sc. Thesis*, Louisiana State University, Baton Rouge, LA., USA.
- Macnaughton, S.J., J.R. Stephen, A.D. Venosa, G.A. Davis, Y-J. Chang, and D.C. White. 1999. Microbial population changes during bioremediation of an experimental oil spill. *Appl. Environmental Microbiol.* ,65(8), 3566-3574.
- Mermillod-Blondin, F., Gaudet, J.-P., Gerino, M., Desrosiers, G., Jose, J., Creuzé des Chatelliers, M. 2004. Relative influence of bioturbation and predation on organic matter processing in river sediments: a microcosm experiment. *Freshwater Biology*, 49, 895-912.
- Mihelcic, J. R. and R.G. Luthy. 1988. Degradation of polycyclic aromatic hydrocarbon compounds under various redox conditions in soil-water systems. *Applied and Environmental Microbiology*, 54, 1182-1187.
- Millward, R.N., Fleeger, J.W., Reible, D.D., Keteles, K.A., Cunningham, B.P., and Zhang, L. 2001. Pyrene bioaccumulation, effects of pyrene exposure on particle-size selection, and fecal pyrene content in the oligochaete *Limnodrilus hoffmeisteri* (tubificidae, oligochaeta). *Environmental Toxicology and Chemistry*, 20, 1359-1366.

Muller, A.K., Westergaard, K., Christensen, S. and S.J. Sorensen. 2002. The diversity and function of soil microbial communities exposed to different disturbances. *Microbial Ecology*, 44, 49-58.

Myers, C.R., Alatalo, L.J., Myers, J.M. 1994. Microbial potential for the anaerobic degradation of simple aromatic compounds in sediments of the Milwaukee Harbor, Green Bay and Lake Erie. *Envir. Toxic. Chem.*, 13, 461-471.

Nakatsu, C., Torsvik, V. and L. Ovreas. 2000. Soil community analysis using DGGE of 16S rDNA polymerase chain reaction products. *Soil Sci. Soc. Am. J.*, 64, 1382-1388.

Pardue, J.H., DeLaune, R.D., and W. H. Patrick, Jr. 1988. Effect of sediment pH and oxidation-reduction potential on PCB mineralization. *Water, Air, and Soil Pollution*, 37, 439-447.

Penry, D.L., Weston, D.P. 1998. Digestive determinants of benzo[*a*]pyrene and phenanthrene bioaccumulation by a deposit-feeding Polychaete. *Environmental Toxicology and Chemistry*, 17, 2254-2265.

Reible, D.D., Popov, V., Valsaraj, K.T., Thibodeaux, L.J., Lin, F., Dikshit, M., Todaro, M.A., and Fleeger, J.W. 1996. Contaminant fluxes from sediment due to tubificid oligochaete bioturbation. *Water Research*, 30, 704-714.

Spencer, D.R. 1980. The aquatic oligochaeta of the St. Lawrence Great Lakes Region. In Brinkhurst, R.O. and D.G. Cook, eds. *Aquatic Oligochaete Biology*. Plenum Press, New York, USA, pp 115-164.

Steif, P. and de Beer, D. 2002. Bioturbation effects of *Chironomus riparius* on the benthic N-cycle as measured using microsensors and microbiological assays. *Aquatic Microbial Ecology*, 27, pp 175-185.

Steffen, K.T., Hatakka, A. and M. Hofrichter. 2003. Degradation of benzo(a)pyrene by the litter-decomposing basidiomycete *Stropharia coronilla*: Role of manganese peroxidase. *Applied and Environmental Microbiology*, 69, 3957-3964.

Sutherland, J.B., Rafii, F., Khan, A.A., and C.E. Cerniglia. 1995. Mechanisms of polycyclic aromatic hydrocarbon degradation, pp. 269-306. In L.Y. Young and C.E. Cerniglia (eds.), *Microbial transformation and degradation of toxic organic chemicals* – 1995. John Wiley & Sons, Inc., New York.

Thibodeaux, L.J. 1996. *Chemodynamics*, 2nd ed., Wiley Interscience, New York, USA.

Thomas, J.M., Yordy, J.R., Amador, J.A., and M. Alexander. 1986. Rates of dissolution and biodegradation of water-insoluble organic contaminants. *Applied Environmental Microbiology*, 52, 290-296.

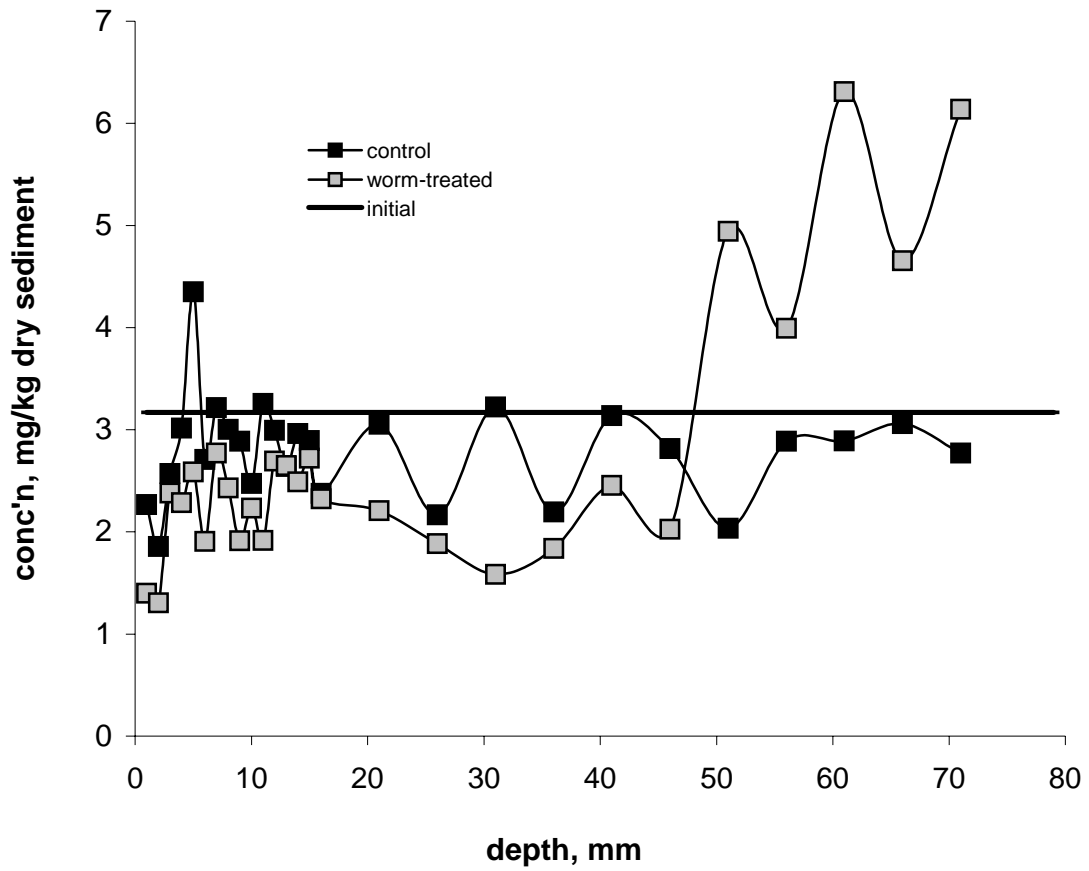
Wang, Xu-Chen, Zhang, Y-X., R.F. Chen. 2001. Distribution and partitioning of polycyclic aromatic hydrocarbons (PAHs) in different size fractions in sediments from Boston Harbor, United States. *Marine Pollution Bulletin* 42,1139-1149.

Weston, D.P., Penry, D.L., Gulmann, L.K. 2000. The role of ingestion as a route of contaminant bioaccumulation in a deposit-feeding polychaete. *Archives of Environmental Contamination and Toxicology*, 38, 446-454.

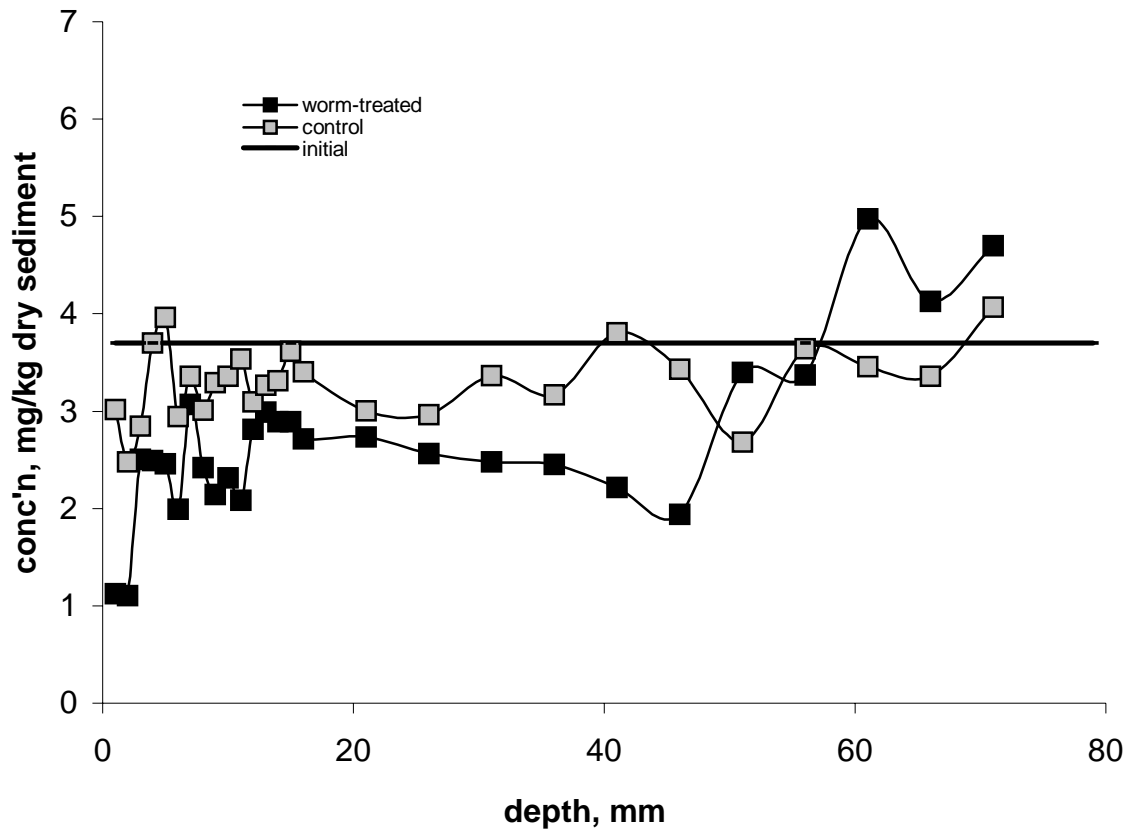
Wattiau, P. 2002. Microbial aspects in bioremediation of soils polluted by polyaromatic hydrocarbons. In: Agathos, S.N., and W. Reineke, editors. *Biotechnology for the Environment: Strategy and Fundamentals*. Kluwer Academic Publishers, Netherlands. pp 69-89.

Zhang, X. and L.Y. Young. 1997. Carboxylation as an initial reaction in the anaerobic metabolism of naphthalene and phenanthrene by sulfidogenic consortia. *Applied and Environmental Microbiology*, 63, 4759-4764.

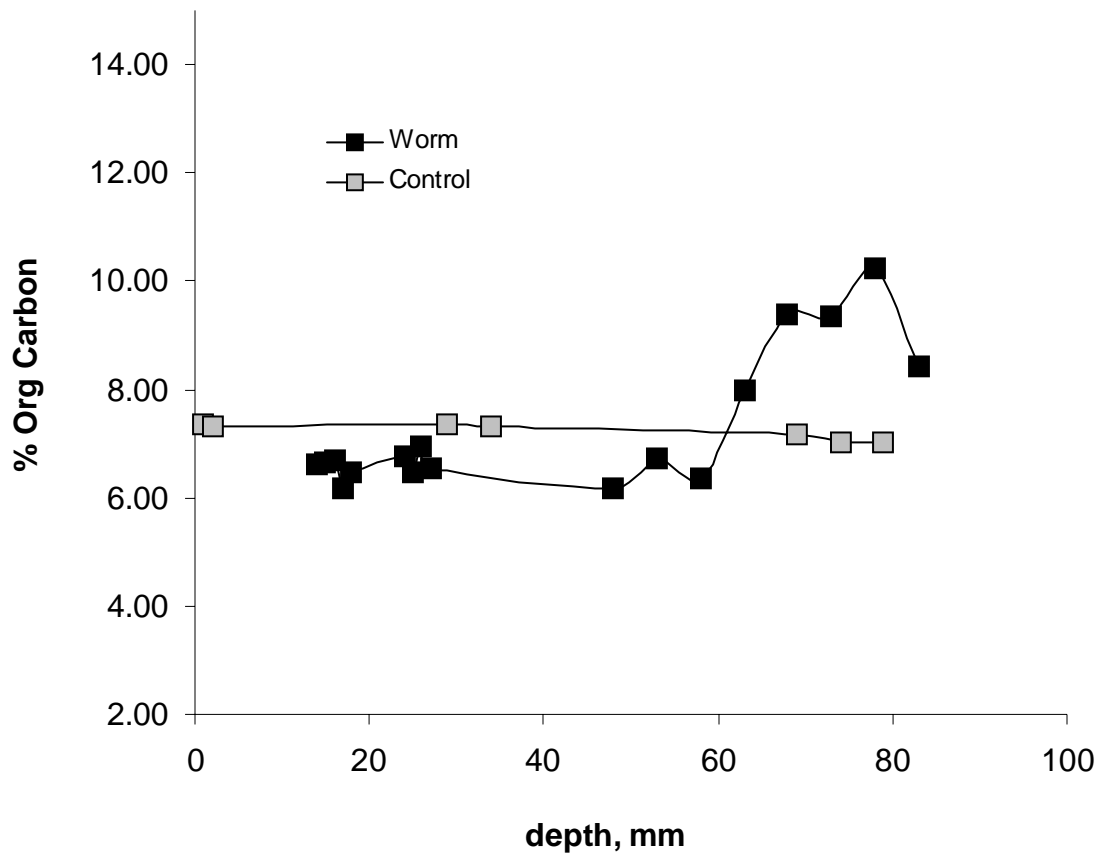
APPENDIX:
RESULTS OF PRELIMINARY SAMPLING



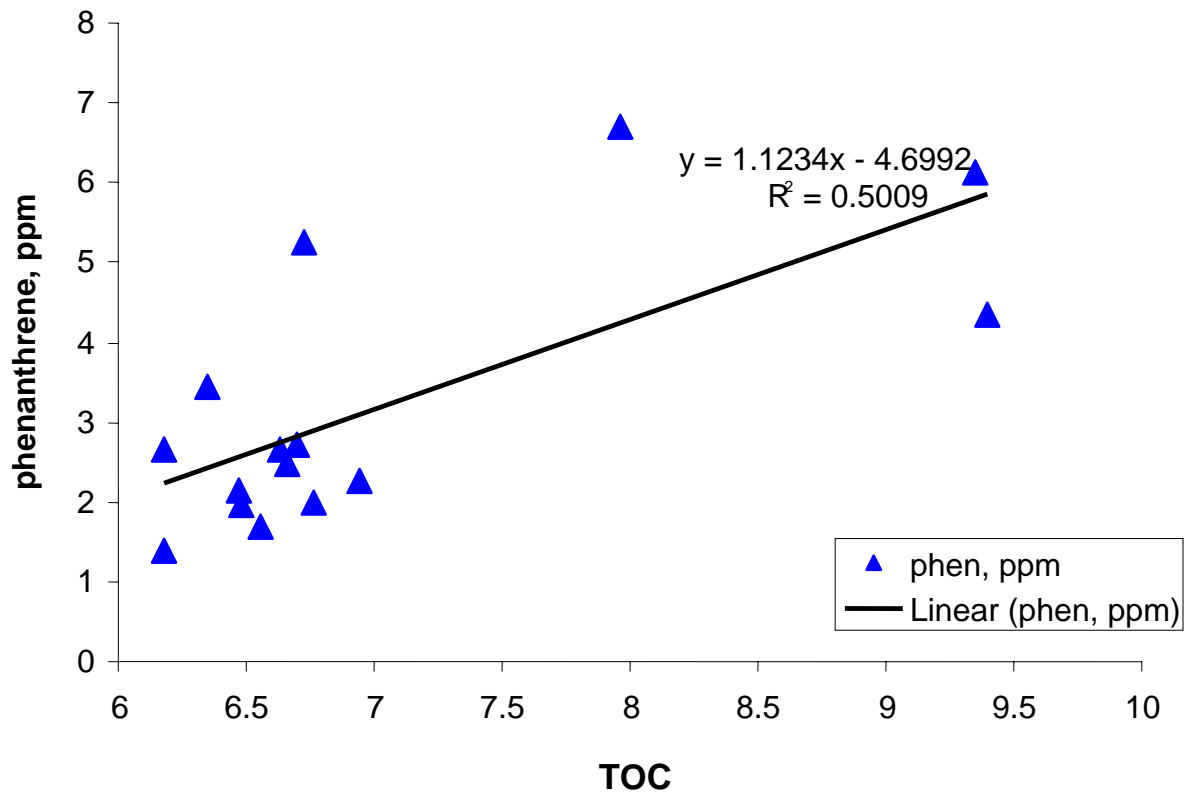
Appendix A-1. Phenanthrene profile obtained from a single control and worm-treated microcosm during a preliminary coring (September, 2004).



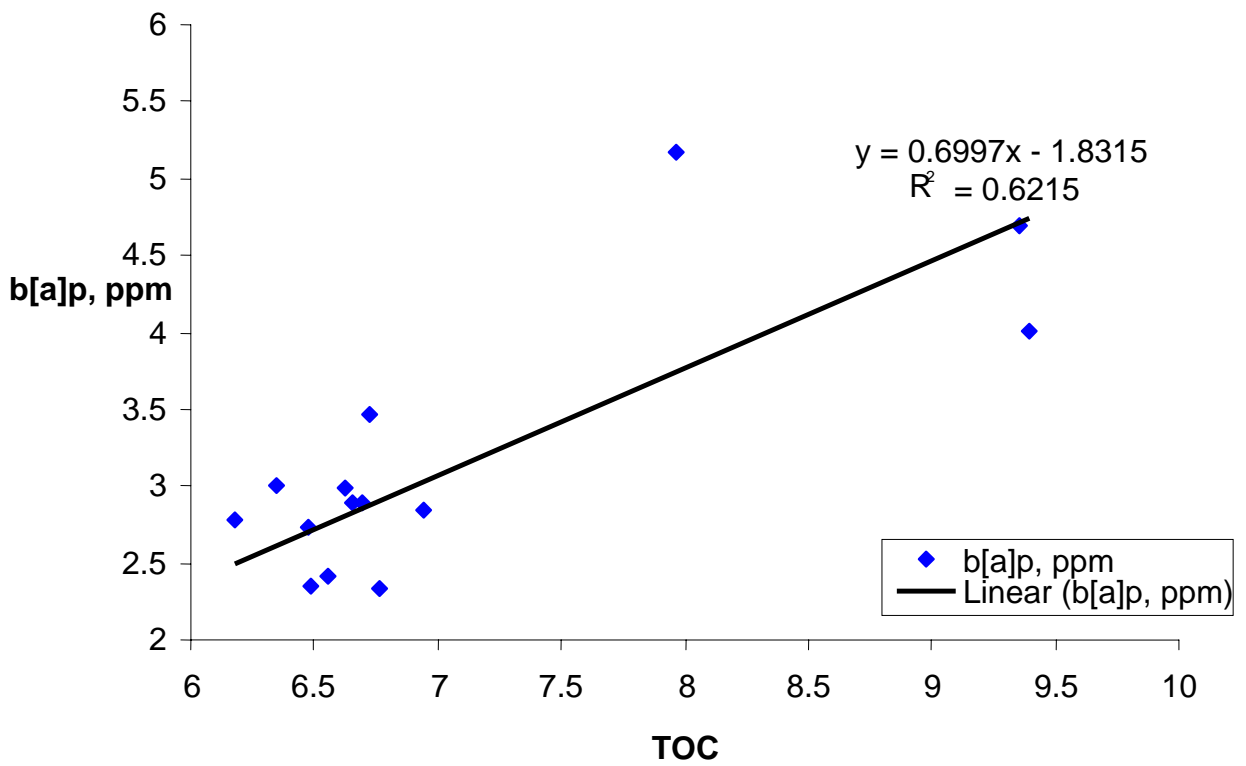
Appendix A-2. Benzo(a)pyrene profile obtained from a single control and worm-treated microcosm during a preliminary coring (September, 2004).



Appendix A-3. Sediment organic carbon (TOC) in a single control and a worm-treated microcosm during a preliminary coring (September, 2004). TOC of original sediment is $6.92 \pm 0.11\%$.



Appendix A-4. Correlation of phenanthrene with sediment organic carbon (TOC) in a worm-treated microcosm during a preliminary coring (September, 2004). TOC of original sediment is $6.92 \pm 0.11\%$.



Appendix A-5. Correlation of benzo[a]pyrene with sediment organic carbon (TOC) in a worm-treated microcosm during a preliminary coring (September, 2004). TOC of original sediment is $6.92 \pm 0.11\%$.

VITA

Marilou Montevirgen Nabatilan is the first child born to Mr. And Mrs. Marcos Romulo Montevirgen on July 12, 1969, in Zambales, Philippines. She took up her bachelor of science in chemical engineering studies from the University of the Philippines, Los Baños (UPLB), and graduated in 1992. Soon after graduation, she served as an Instructor in Physics in UPLB for one year. She then got married to a college classmate, Larry Nabatilan and had their first child, their daughter – Arielle Madison. Through the joys and hardships of motherhood, she pursued her master’s degree in environmental engineering at the University of the Philippines, Diliman, during which she had two sons – Joshua Lawrence and Miguel Adrian Nabatilan. She also went back to teaching, joining the faculty of the Institute of Chemistry, UPLB in 1996-1997. Since 1997, she had been with the Department of Chemical Engineering, UPLB.

She came to LSU in Fall, 2002, and is now working toward a doctoral degree in civil engineering. Meanwhile, the Master of Science in Chemical Engineering shall be conferred on her in December, 2005.